In presenting the dissertation as a partial fulfillment of the requirements for an advanced degree from the Georgia Institute of Technology, I agree that the Library of the Institute shall make it available for inspection and circulation in accordance with its regulations governing materials of this type. I agree that permission to copy from, or to publish from, this dissertation may be granted by the professor under whose direction it was written, or, in his absence, by the Dean of the Graduate Division when such copying or publication is solely for scholarly purposes and does not involve potential financial gain. It is understood that any copying from, or publication of, this dissertation which involves potential financial gain will not be allowed without written permission.

J D A

3/17/65
b

AN INVESTIGATION OF TRANSIENT FREE CONVECTION INSIDE A HORIZONTAL CYLINDER BY MEANS OF DIFFERENTIAL INTERFEROMETRY

A THESIS

Presented to

The Faculty of the Graduate Division

by

Gene L. Spence

In Partial Fulfillment

of the Requirements for the Degree

Master of Science in Mechanical Engineering

Georgia Institute of Technology

June, 1968

AN INVESTIGATION OF TRANSIENT FREE CONVECTION INSIDE A HORIZONTAL CYLINDER BY MEANS OF DIFFERENTIAL INTERFEROMETRY

Approved:

Chairman

Date approved by Chairman: 4/22/68

ACKNOWLEDGEMENTS

The author would like to express his appreciation to those who have contributed their help and encouragement to this work. The author is very grateful to Dr. Walter O. Carlson, the faculty advisor for this thesis, whose understanding and professional guidance have led to the completion of this work. The constructive comments and time given by the reading committee, Dr. C. W. Gorton and Dr. P. Durbetaki, are gratefully acknowledged.

The author would also like to especially thank Mr. L. C. Prowse and Mr. B. T. Hendricks who have offered much helpful advice and assistance in the photography of this work.

Finally, the author would like to express sincere appreciation to his wife for her continued support and understanding.

TABLE OF CONTENTS

Page

ACKNOWLEDGEMENTS ii

LIST OF TABLES v

LIST OF ILLUSTRATIONS vi

SUMMARY vii

NOMENCLATURE ix

Chapter

I. INTRODUCTION 1

II. DIFFERENTIAL INTERFEROMETER THEORY 4

Description
Analysis of Interferograms

III. EQUIPMENT 16

Differential Interferometer
Test Cylinder
Heating Element
Temperature Measuring System
Photographic System

IV. PROCEDURE 24

V. RESULTS 27

VI. CONCLUSION 38

TABLE OF CONTENTS (Cont.)

Page

APPENDICES

1. REDUCTION OF INTERFEROGRAMS 39

2. CALIBRATION OF THERMOCOUPLES 48

3. ERROR ANALYSIS 49

BIBLIOGRAPHY 51

LIST OF TABLES

Table		Page
1.	Index of Refraction vs. Temperature	13
2.	Filter Data	19
3.	Wollaston Prism Data	19
4.	Sequence of Photographs	26
5.	Calibration of Thermocouples	48

LIST OF ILLUSTRATIONS

Figure		Page
1.	Research Equipment	3
2.	Schematic Diagram of Mach-Zehnder Interferometer	5
3.	Schematic Diagram of Differential Interferometer	6
4.	Interferogram for a Straight Solid Boundary	10
5.	Interferogram for a Curved Solid Boundary	11
6.	Differential Interferometer	17
7.	Transient Wall Temperature	25
8.	Isotherms - τ = 90 sec.	29
9.	Isotherms - τ = 120 sec.	30
10.	Isotherms - τ = 180 sec.	31
11.	Isotherms - τ = 240 sec.	32
12.	Isotherms - τ = 300 sec.	33
13.	Isotherms - τ = 360 sec.	34
14.	Isotherms - τ = 720 sec.	35
15.	Isotherms - τ =1200 sec.	36
16.	Transient Bulk Temperature	37
17.	Transient Center Temperature	43
18.	Typical Vertical (90°) Interferogram	44
19.	Typical Vertical Interferogram Evaluation Results . . .	45
20.	Typical Transient Temperature at a Horizontal Fringe Position	46
21.	Typical Horizontal (0°) Interferogram	47

SUMMARY

An optical device, called a differential interferometer, which can be used for recording temperature has been developed in France. After assembling a differential interferometer, an operating procedure was developed for its use. The differential interferometer was then applied to a two-dimensional, transient, laminar, free convection heat transfer problem. The output of the differential interferometer is in the form of interference fringe patterns (interferograms). It was necessary to develop a new technique for evaluation of the interferograms when the differential interferometer was applied to the following experimental study.

Tests were run of transient, laminar, free convection inside a horizontal, water-filled, cylinder under the condition of constant wall temperature greater than the initial uniform temperature of the water by 3.0°F. After the test began, the interferograms were reordered on 35 mm. Kodachrome II film at various times. These interferograms were then processed by hand and presented in the form of isotherms of the water-filled cavity as a function of time.

In each interferogram the position of the wall and the position of the deflected fringes at the wall had to be approximated due to irregularities in the cylinder diameter, misalignment of the rubber gaskets, and appearance of a double image of the cylinder, a phenomenon basic to all differential interferometers. Due to the location of the horizontal fringes, no data were available either at the top or at the

bottom of the cylinder. The heat transfer phenomenon is characterized by a region approaching pure conduction close to the wall and a region of free convection along the vertical centerline. After approximately thirty minutes the temperature of the water had asymptotically reached that of the wall, resulting in a cessation of heat transfer. The isotherms were evaluated to obtain transient bulk temperatures.

Results of this research indicate that the differential interferometer can be used in problems characterized by confining solid boundaries. The technique developed for evaluating interferograms for curved solid boundaries proved valid.

NOMENCLATURE

Symbol

A	=	area
D	=	fringe spacing
d	=	known linear distance
g	=	focal length of the concave mirrors in the instrument
$\bar{h}$	=	average film coefficient of heat transfer
ℓ	=	length of the test cylinder
MF	=	magnification factor
m	=	dimensionless fringe deflection
n	=	index of refraction
REF	=	reference boundary
T	=	temperature
x	=	distance measured along an axis parallel to undeflected fringe direction
y	=	distance measured along an axis parallel to curved wall of cylinder
φ	=	optical path
θ	=	$T - T_{H_2O\text{-INITIAL}}$
ϕ	=	wedge angle of Wollaston-Prism
λ	=	wavelength of light
τ	=	time
ΔX	=	beam separation distance

Subscripts

BULK	=	bulk or average value
e	=	extraordinary
o	=	ordinary
H_2O-CENTER	=	temperature at the center of the cylinder
H_2O-INITIAL	=	initial uniform water temperature
HORIZ.	=	horizontal
T.C.	=	thermocouple
VERT.	=	vertical
w	=	wall

CHAPTER I

INTRODUCTION

The technique of differential interferometry was discovered by Renet (1) in France in 1954. The original and most frequent applications of differential interferometry have been in the field of aerodynamics (2-10). In heat-transfer Regnier and Kaplan (11) applied differential interferometry to free convection in transitional and turbulent regimes on a plane wall and in a vertical gap. Lamb and Schreiber (12) applied differential interferometry to an axially symmetric arc heated plasma.

A differential interferometer manufactured by Feinmechanik und Optik in Wenden, West Germany, was assembled for use in this research. Next, the instrument was studied to develop an operating procedure which could be applied in future research with this differential interferometer. This study determined the necessary adjustments which must be made in each experimental investigation.

This differential interferometer was then applied to a type of problem different from that of references 2-12. References 2-12 can be characterized as external geometry rather than internal geometry problems. Characteristically, references 2-12 are external in that the accompanying fluid movement is over the solid boundaries and is not confined by them. A characteristically internal geometry problem, one with confining solid boundaries, was chosen for this investigation.

Transient free convection in a horizontal cylinder has been investigated by Hellums and Churchill (13). Using both air and water and starting with the fluid initially at rest at a uniform temperature, Hellums and Churchill (13) maintained the opposing vertical walls of the cylinder at different uniform temperatures with one wall serving as a heat source and the other wall serving as a heat sink until velocity, temperature, and heat transfer parameters no longer changed with time (steady state). Hellums and Churchill (13) presented a numerical solution to this problem which agreed quite well with their experimental results and which also approached the steady state results of the same problem presented by Martini and Churchill (14) using air.

In this research transient, laminar, free convection inside a long, horizontal, water-filled cylinder under the condition of constant wall temperature greater than the initial uniform temperature of the water by 3.0°F was investigated by means of differential interferometry. As a part of this investigation it was necessary to develop a new technique for evaluation of the interference-fringe deflection patterns, interferograms, produced in the instrument by the heated test cylinder. This new evaluation technique was a result of the confining walls being curved rather than straight as in references 2-12.

The temperature distributions in the cylindrical water-filled cavity were obtained from the differential interferometer as a function of time. Figure 1 shows the test cylinder and differential interferometer used in the research.

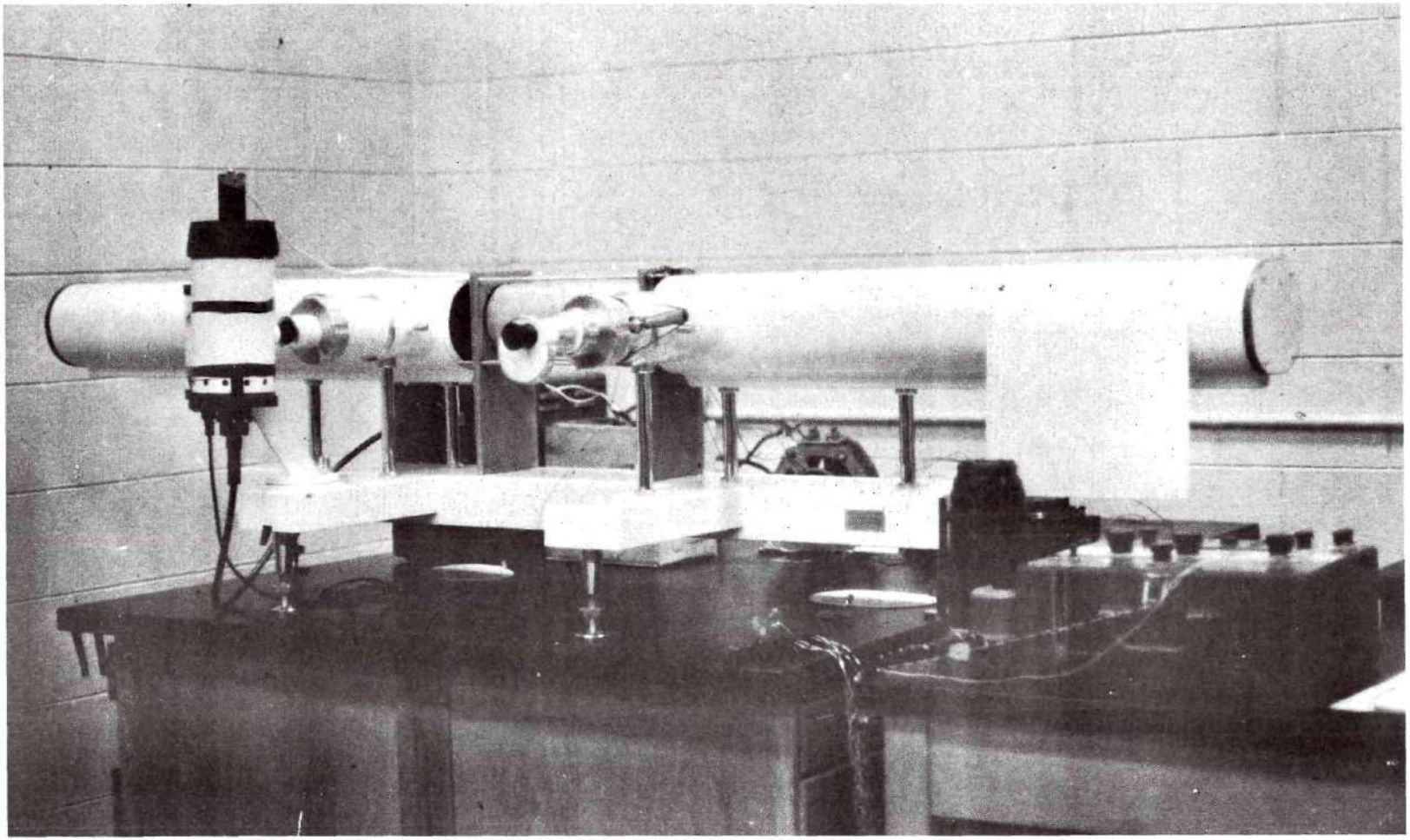

Figure 1. Research Equipment

CHAPTER II

DIFFERENTIAL INTERFEROMETRY

Description

A differential interferometer is an optical device which permits the determination of temperature distributions in heat transfer work from deflected fringe patterns called interferograms which are produced by the instrument.

The vast majority of heat transfer work by interferometry has been accomplished with the classical Mach-Zehnder interferometer. Wilkie and Fisher (15) have presented a comprehensive paper on temperature measurement by Mach-Zehnder interferometry.

The Mach-Zehnder interferometer, Figure 2, provides two widely separated paths for the light between the source and the point at which the two beams are combined. The test beam passes through the test section while the reference beam from the same source simultaneously passes around the test section and through an undistributed region.

In contrast, the differential interferometer, Figure 3, has no reference beam. A single beam of light is split into two closely spaced beams by the differential interferometer.

Thus, the Mach-Zehnder interferometer, having a constant reference beam, gives a continuous variation in temperature from the reference. The differential interferometer, having by comparison closely spaced beams, has no fixed reference. These closely spaced beams travel slight-

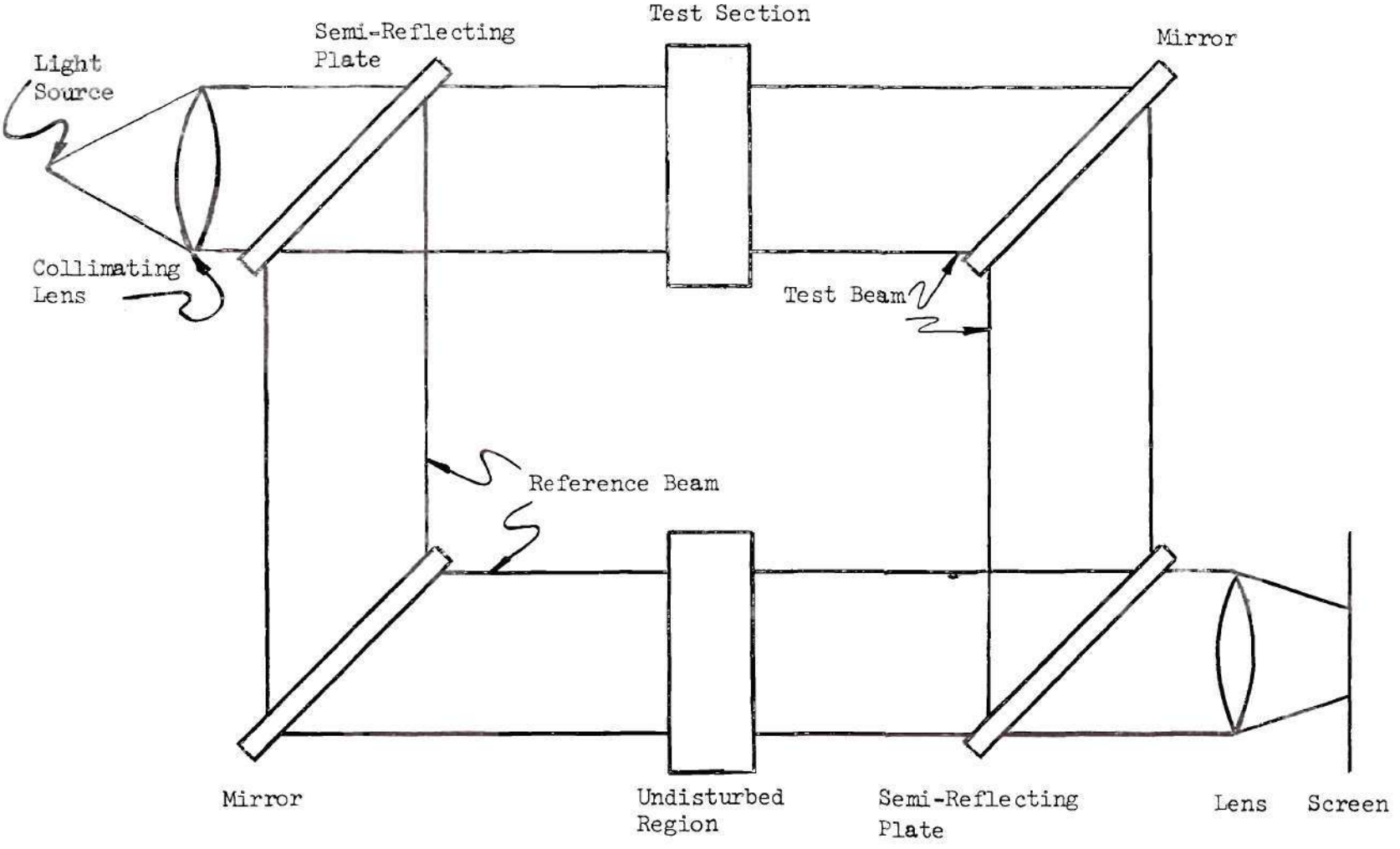

Figure 2. Schematic Diagram of Mach-Zehnder Interferometer

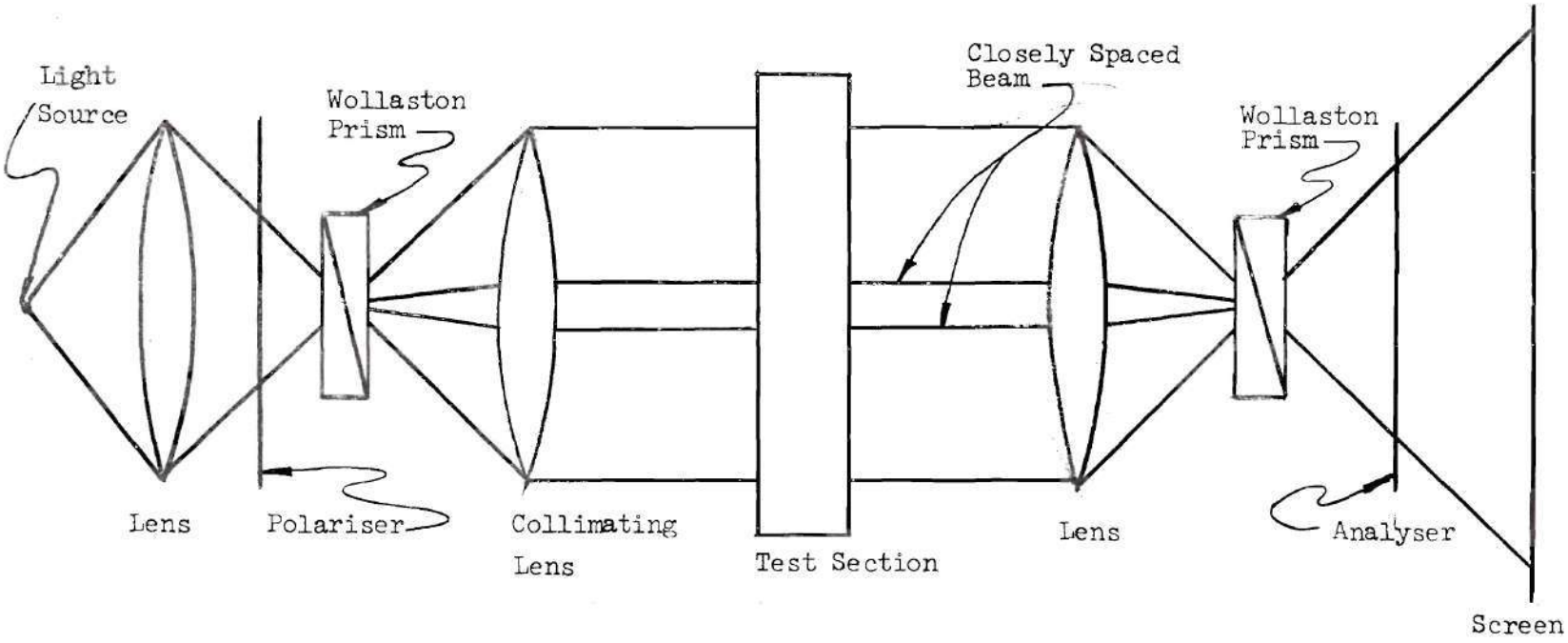

Figure 3. Schematic Diagram of Differential Interferometer

ly different paths through the test section. The differential interferometer therefore gives a point-to-point variation of temperature in the test section.

Lamb and Schreiber (12) present a detailed discussion of the theory of differential interferometry and the mechanism by which the single beam of light is split into the two closely spaced beams. Basically, light from a nearly monochromatic source passes through a polariser which polarises the ray at 45° to the optic axis of the Wollaston Prism, thus giving equal intensities to both the ordinary and extraordinary rays produced in the Wollaston Prism. The ordinary and extraordinary rays produced in the Wollaston Prism are plane polarised in mutually perpendicular directions and are separated by the small lateral displacement ΔX. The two rays traverse the test section separated by ΔX and enter the next Wollaston Prism where the splitting action of the first prism is compensated. The analyser brings the two wave fronts emerging from the second prism into the same plane of polarization for interference to take place.

Analysis of Interferograms

The output of the differential interferometer is in the form of interference fringe patterns (interferograms). These interferograms provide the means for relating the desired variable, temperature, to the instrument parameter, fringe deflection. Lamb and Schreiber (12) derive the following equation relating the optical path, φ, of which temperature is a function, to the fringe deflection, m.

$$\varphi(x) = \frac{\lambda}{\Delta X} \int_{REF}^{x} m(x)\, dx \qquad (1)$$

The optical path, φ, is defined by

$$\varphi \equiv n.\ell \tag{2}$$

where n is the index of refraction of the medium under consideration and ℓ is the length of the test section along a direction parallel to the light rays. The wavelength of the monochromatic light used is λ and ΔX is the beam separation distance. Both λ and ΔX are constants of the differential interferometer. The fringe deflection of the interferograms from the original undeflected fringe position is m(x) and is measured in units of fringe spacing. The direction perpendicular to the light beams is x. Integration proceeds from a reference boundary, REF, where conditions must be known to any point x.

In the free convection heat transfer problem under investigation the length of the test cylinder, ℓ, is constant.

Substituting Equation (2) into Equation (1)

$$\varphi(x) = n(x).\ell = \frac{\lambda}{\Delta X} \int_{REF}^{x} m(x)\, dx \tag{3}$$

and

$$n(x) = \frac{\lambda}{\Delta X.\ell} \int_{REF}^{x} m(x)\, dx \tag{4}$$

The fringe deflection, m(x), measured in dimensionless units of fringe spacing, can be written

$$m(x) = \frac{y(x)}{D} \tag{5}$$

where D is the fringe spacing, a constant of the instrument measured on the undeflected interferogram, and y(x) is the fringe deflection measured in the same linear dimension as D.

Substituting Equation (5) into Equation (4)

$$n(x) = \frac{\lambda}{\Delta X \cdot \ell \cdot D} \int_{REF}^{x} y(x)\, dx \qquad (6)$$

Knowing λ, ΔX, ℓ, and D as constants for a particular instrument and test set-up, all that remains in Equation (6) is to evaluate the integral. Figures 4 and 5 identify the integral.

Figure 4 is an interferogram for a straight solid boundary. It is seen that the integral in Equation (6) represents the area between the deflected and undeflected fringe position. Figure 4 is typical of the previous applications of differential interferometry, references 2-12.

Figure 5 is an interferogram for a curved solid boundary, a situation not encountered in references 2-12. It was experimentally determined during this research that the deflection of the fringe, y(x), from its undeflected position, should be measured along an arc having the same center as the curved solid boundary. Given a straight solid boundary and a curved solid boundary, with the same Δn from some reference boundary to the wall, the total area under each deflected fringe (straight and curved solid boundaries) has to be equal to satisfy Equation (6). It is the point-to-point variation of n that necessitates the measurement of y(x) along the curved arc. The measurement of y(x) along the curved arc was determined by the following reasoning. In Figure 4 it is

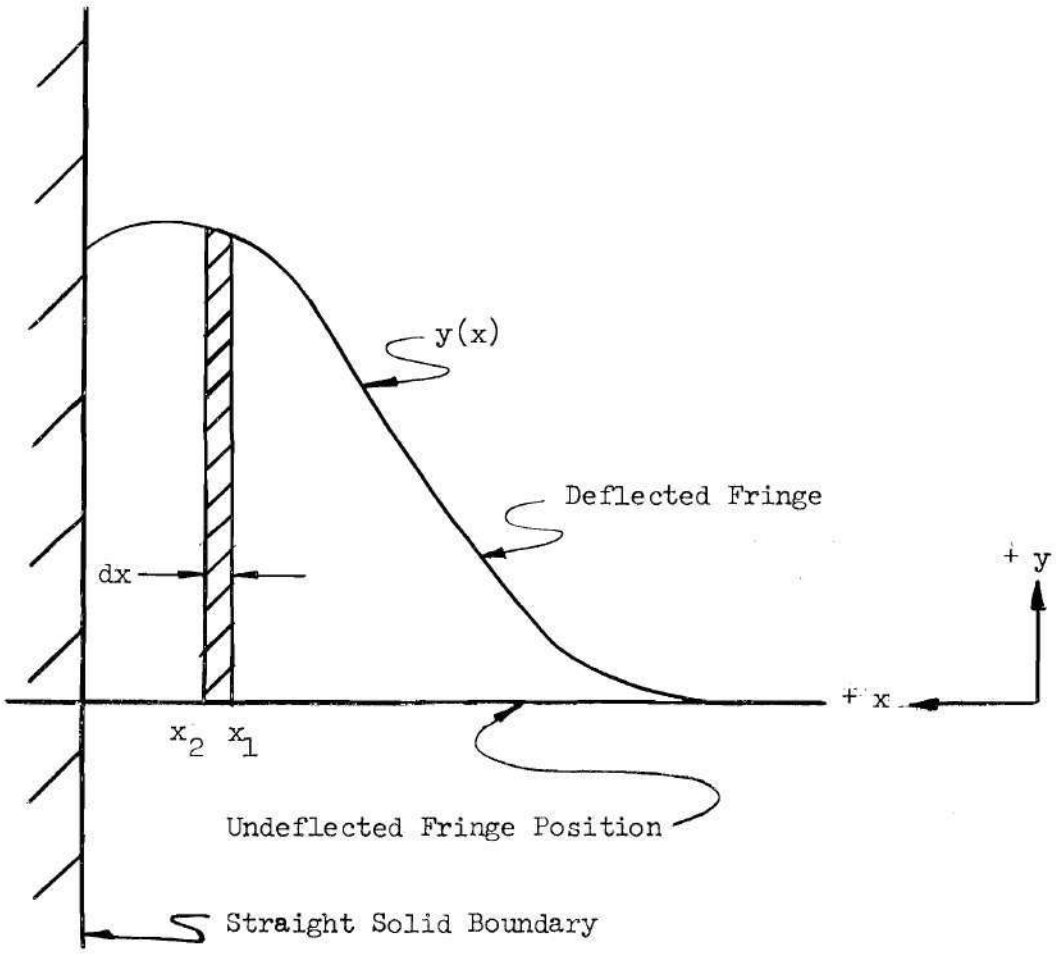

Figure 4. Interferogram for a Straight Solid Boundary

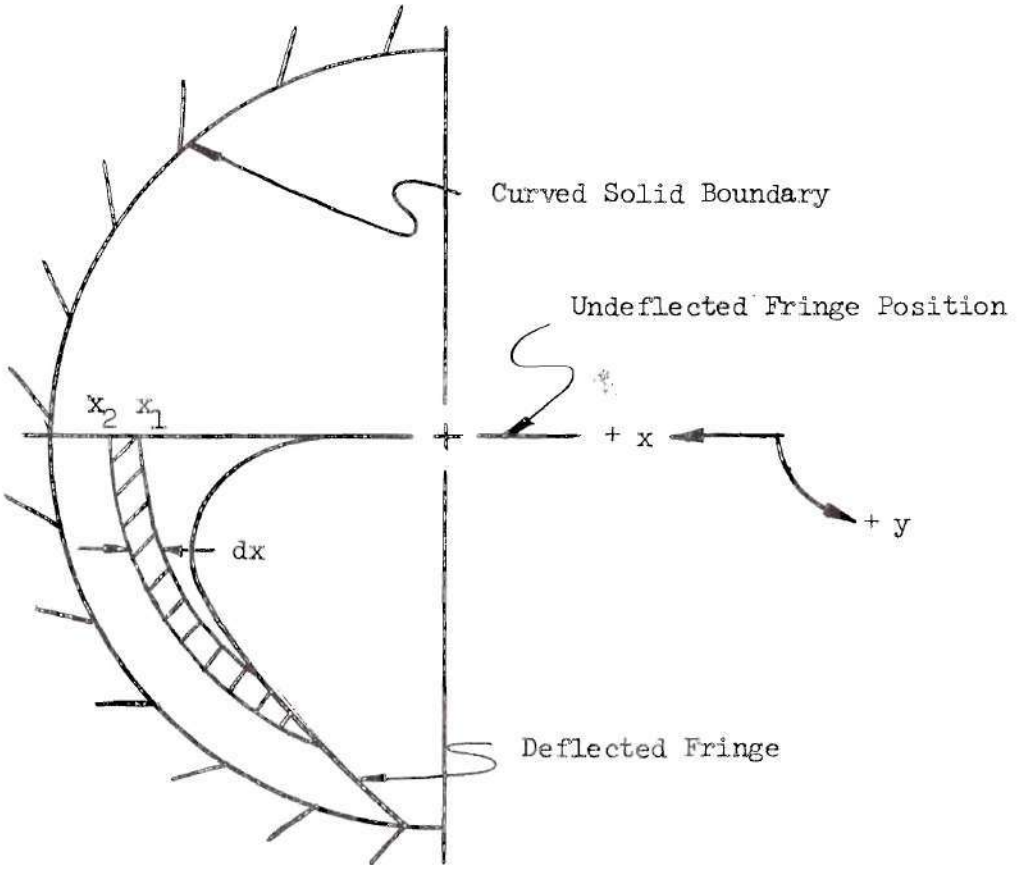

Figure 5. Interferogram for a Curved Solid Boundary

seen that the defining lines for the value of $y(x)$ at both point x_1 and point x_2 are parallel to the straight boundary. As shown in Figure 5, the defining lines for the value of $y(x)$ at both point x_1 and x_2 were made parallel to the curved boundary. Evaluation of a typical interferogram produced realistic results and the technique was adopted.

Note that in Equation (6) the integration proceeds from a reference boundary, REF, where the index of refraction (temperature) must be known. For the case shown in Figure 5 the reference boundary was chosen for convenience to be the center of the cylinder. Other tests may warrant use of another reference such as the wall.

As it stands, Equation (6) presents the distribution of the index of refraction within the cylinder. It now remains to correlate the desired variable, temperature, with the calculated parameter, index of refraction.

The index of refraction is shown by Weinberg (16) to be a function of composition, pressure, wavelength, and temperature.

In the water-filled, cylindric cavity under investigation the composition of the water does not vary. Pressure variation in this research is negligibly small and, thus, does not affect n. The light source is nearly monochromatic (λ = constant) due to the presence of a narrow bandpass filter in the differential interferometer. Thus, the index of refraction is seen to be a function of temperature only. Tabulations of the variation of index of refraction with temperature at a given wavelength have been made by Dorsey (17) and are presented in Table 1.

One final note in the evaluation of Equation (6) concerns magni-

Table 1. Index of Refraction vs. Temperature

T(C)	10	20	30	40	15	25	35
λ(Å)	n				$-(10^6)\frac{\Delta n}{\Delta T}$		
5876	1.333744	1.333041	1.331993	1.330662	70.7	105.0	133.2
5770	1.334085	1.333380	1.332331	1.330998	70.9	105.2	133.5
5461	1.335176	1.334466	1.333411	1.332071	71.4	105.8	134.1
5016	1.337070	1.336353	1.335289	1.333939	72.1	106.7	135.2
4861	1.337842	1.337123	1.336055	1.334702	72.3	107.0	135.4
4713	1.338653	1.337931	1.336860	1.335504	72.6	107.3	135.8
4476	1.340149	1.339423	1.338347	1.336984	73.0	107.8	136.5
4358	1.340938	1.340210	1.339131	1.337765	73.2	108.1	136.8

fication factors. Photographs of deflected fringe patterns (interferograms)can be enlarged to any practical size to increase the accuracy of the integration process in Equation (6) and Figure 5. This enlargement does not affect λ, ΔX, and ℓ in Equation (6). It does, however, affect D and the integral which is represented by an area, A. The magnification factor, MF, is defined by

$$MF \equiv \frac{d_{photo}}{d_{actual}} \tag{7}$$

where d is some known linear distance which always appears in the photographed interferograms. In the interferograms produced in this research the known distance is taken to be the inside diameter of the cylinder.

Equation (6) can be written

$$n(x)_{actual} \propto \frac{A_{actual}}{D_{actual}} \tag{8}$$

It is easily seen that

$$A_{actual} = \frac{A_{photo}}{(MF)^2} \tag{9}$$

and

$$D_{actual} = \frac{D_{photo}}{MF} \tag{10}$$

Substituting Equations (9) and (10) into (8)

$$n(x)_{actual} \propto \frac{A_{photo}}{D_{photo}} \Big/ MF \tag{11}$$

Therefore, Equation (6) can be written for the photographed interferograms as

$$n(x) = \frac{\lambda}{\Delta X \cdot \ell \cdot D \cdot MF} \int_{REF}^{x} y(x)\, dx \tag{12}$$

CHAPTER III

EQUIPMENT

The systems necessary to carry out this research were divided into five main areas. These areas were:

1. Differential interferometer
2. Test cylinder
3. Heating element
4. Temperature measuring system
5. Photographic system

Differential Interferometer

The differential interferometer used in this research was manufactured by Feinmechanik und Optik, Weden, West Germany. A brochure (19) included with this instrument presents the operating procedure and brief theory of the differential interferometer. Lamb and Schreiber (12) completely describe the theory and operation of a similar differential interferometer.

Figure 6 shows the differential interferometer used in this research. This instrument has a field vision of 3-3/4 in. diameter and can accommodate test setups of up to 16 in. in length.

There are five major settings of the interferometer required for each test run. Three of these settings are concerned with the three instrument constants in Equation (12).

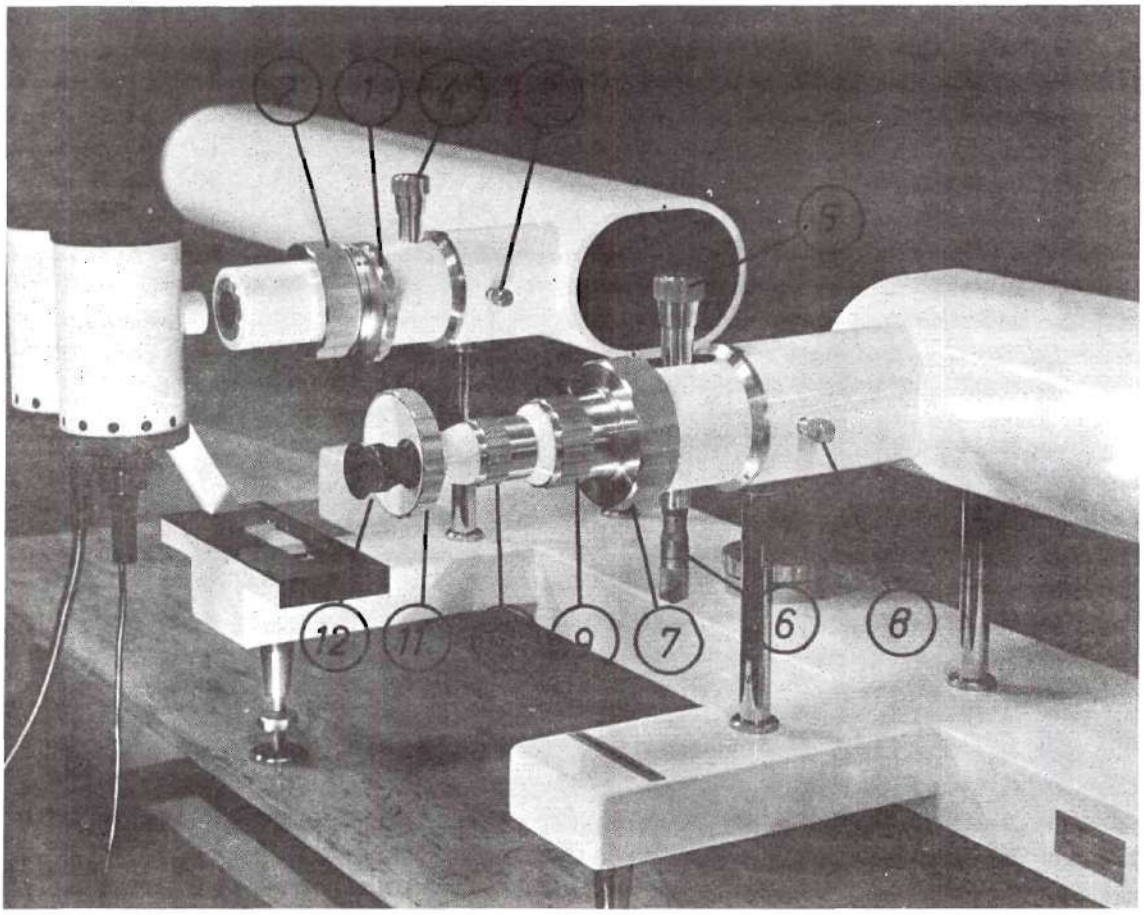

Figure 6. Differential Interferometer

First, there are two light sources. A 12 V-40 watt bulb (projector type) OSRAM No. 8024, is used for viewing tests through the instrument eyepiece. A high pressure mercury lamp, OSRAM HBO 200 W/2, 120 V, Li, is used for either photographing or projecting the interferograms on a screen. The high intensity mercury lamp is ideal for photographing transient phenomena where high shutter speeds are required.

The second instrument setting fixes the value of λ, the wavelength of the light used. Three narrow bandpass interference-fringe filters are provided for use with this instrument. Filter parameters are listed in Table 2.

The third instrument setting fixes the value of ΔX, the beam separation distance. Lamb and Schreiber (12) show that

$$\Delta X = 2g(n_e - n_o) \tan \phi \qquad (13)$$

The focal length of the built-in concave mirrors of the instrument is g, a constant, and equals 100 cm. The difference in index of refraction for the ordinary and extraordinary rays through quartz, Halliday and Resnick (18), is $(n_e - n_o)$ a constant, and equals 0.009165. Equation (13) can now be written

$$\Delta X = 0.0602 \tan \phi \qquad (14)$$

with the units of ΔX being feet.

The wedge angle of the Wollaston Prism used in the instrument is ϕ. There are three Wollaston Prisms with different values of ϕ which are listed in Table 3 along with the corresponding values of ΔX

Table 2. Filter Data

Color	Blue	Green	Orange
λ (Å) (Center of Peak Transmission)	4400	5440	5820
Peak Transmission (Per Cent)	38	38	35
Narror Bandpass (Å)	120	120	150

Table 3. Wollaston Prism Data

Wollaston Prism Setting Number	ϕ	ΔX(Feet)
0	(No Prism Present)	
1	1°	0.001048
2	3°	0.00315
3	8°	0.00844

from Equation (14). Prism setting zero (0) has no prism present and is used to locate the undeflected fringe position (reference base line, $y = 0$) when evaluating the integral in Equation (12).

The fourth instrument setting fixes the value of D, the fringe spacing. Four different fringe spacings are available, narrow, medium, wide, and infinite, i.e. no fringes. The infinite fringe spacing is used for qualitative observation of the test section. D is measured on the photographed interferograms.

The fifth instrument setting fixes the direction of the undeflected fringe. The undeflected fringes may be oriented at any angle between 0° (horizontal) and 90° (vertical).

In comparison to other optical devices in which a quantitative evaluation is possible such as the Mach-Zehnder interferometer, the differential interferometer is simpler and less expensive. It is easier to set up, operate, and move, and is less subject to vibrations. Its major disadvantage is the accuracy which is lost through the integration process in Equation (12). This integration process is unnecessary in Mach-Zehnder interferometry and, thus, constitutes an additional time-consuming and error-inducing step in the data reduction of differential interferometer interferograms. Appendix 3 presents an analysis of the errors present in this research. An error in the temperature at a point of ± 19.0 per cent is directly attributed to differential interferometry as used in this research.

Test Cylinder

The test cylinder used in this research was aluminum tubing,

3.005 in. outside diameter, by 11.75 in. long by 0.085 in. wall thickness. The ends of the cylinder were machined perpendicular to the axis. Both the inside and outside of the cylinder were sanded, primed, and painted with silver spary enamel to eliminate corrosion. A thermocouple probe hole of 1/16 in. diameter was drilled in the wall at the top of the cylinder 1/4 in. from each end. A silicon rubber heater described in the next section was attached to the outside of the test cylinder. Both the test cylinder and the heater were placed inside a 4 in. IPS by 11.75 in. long cast iron pipe. Preparation of the iron pipe was similar to that of the aluminum cylinder with the exception of drilling an additional hole through the top of the iron pipe wall for the heater lead wires. Ordinary plate glass 7/32 in. thick by 4 in. square was used to enclose the ends of the cylinders. Tests of several pieces of commercial plate glass indicated that variation of their optical thicknesses, φ in Equation (2), was negligible compared to the variation of optical thickness of the heated, water-filled cavity. Rubber gaskets, 1/32 in. thick, provided a good seal between the cylinders and the plate glass.

This entire assembly was then placed between two 1/4 in. thick by 6 in. wide by 12 in. high plywood mounting frames. Four threaded rods 1/8 in. diameter by 14 in. long and mounted at the corners of $4\frac{1}{2}$ in. square centered on a 3-3/4 in. diameter hole passed through the plywood mounting frames and mechanically compressed the glass plates to the cylinders.

A fine jet of water from an ordinary laboratory faucet was then sprayed through the thermocouple probe hole into the large iron pipe. The test cylinder was filled with water by leakage through its thermo-

couple probe hole. The system was then checked to insure that air bubbles were not present.

Heating Element

A silicone rubber heater, 3 in. inside diameter by 11 in. long by 0.055 in. thick, was attached by strips of electrical tape to the outside of the test cylinder. This electrical resistance heater was purchased from Watlow Electric Company of California. Maximum heat output was 5 watts/in^2. for the 115 volt, 60 Hz, single phase heating element. Input to the heater was controlled by a 230 volt, 60 Hz, 9 amp Superior Electric Company Powerstate (voltage transformer).

Before mounting the test cylinder between the plywood frames, a test was made to determine the uniformity of temperature around the test cylinder. The temperature differences (recorded temperature minus ambient temperature) recorded at five stations around the test cylinder each deviated by less than ten per cent from the mean value of the five recorded temperature differences.

Sharply defined fringes indicated that axial variation of wall temperature was negligible. Thus, a two-dimensional test set-up was assured.

Temperature Measurement System

At one end of the test cylinder a thermocouple was inserted at the heater test cylinder interface. At the other end of the test cylinder a thermocouple was positioned at the center of the cylinder 1/4 in. from the end. Calculations showed boundary layer end effects to be negligible at this position. The thermocouples were twenty-gage iron-con-

stantan. All of the temperature-time data collected in the tests were obtained manually using a stopwatch and a Leeds and Northup model 8686 millivolt potentiometer.

Photographic System

The camera used for recording the transient interograms was a 35 mm Nikon mounted on a tripod and focused through the differential interferometer lens. Kodachrome II, Type A film was used in conjunction with the orange filter of the instrument to obtain slides which could then be projected to any size on a screen by means of a slide projector. Projection of the interferograms onto a screen resulted in a slight distortion of the test cylinder shape from a circle into an ellipse. See Appendix 3, for a quantitative evaluation of the effect of this distortion.

CHAPTER IV

PROCEDURE

A wall temperature greater than the initial uniform temperature of the water filled cavity was maintained constant for all time. As shown in Figure 7, a temperature difference of 3.0°F was selected, this value resulting in laminar flow, turbulent flow resulting from higher temperature differences. With an initial setting of 115 volts on the Powerstat around ten seconds were required to bring the wall up to the required temperature. An additional twenty to thirty seconds are required to stabilize this temperature. A typical plot of wall temperature actually obtained is also shown in Figure 7. As time increased, the Powerstat setting was continuously decreased maintaining the required wall temperature.

Several test runs were made without photography to obtain accurate transients of the temperature of the center of the water filled cavity, $T_{H_2O\text{-CENTER}}$. These values form the reference boundary in Equation (12) for each instant of time.

After making the five differential interferometer adjustments discussed in Chapter III, two test runs were photographed according to the sequence listed in Table 4. Both photographed tests used the high pressure mercury lamp, the orange filter, the one degree Wollaston Prism, and the medium fringe spacing. The first photographed test run used an undeflected fringe angle of 90° (vertical) while the second run used an angle of 0° (horizontal).

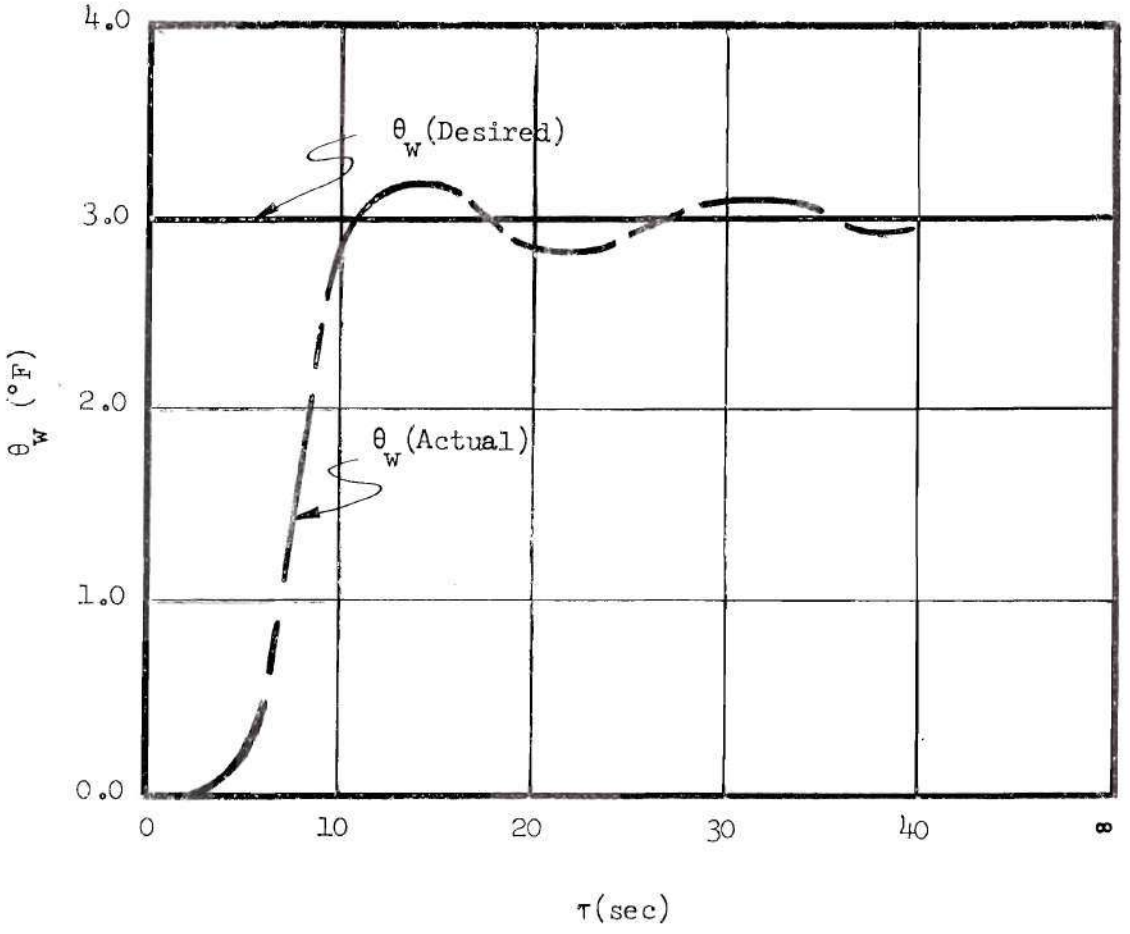

Figure 7. Transient Wall Temperature

Table 4. Sequence of Photographs

Photograph Number	τ(sec)
1 (undeflected fringe position)	0
2 (heating begins)	0
3	10
4	20
5	30
6	40
7	50
8	60
9	70
10	80
11	90
12	120
13	150
14	180
15	240
16	300
17	360
18	720
19	1200
20	1800

CHAPTER V

RESULTS

The interferograms for times of 90, 120, 180, 240, 300, 360, 720, and 1200 sec. were evaluated using the procedure shown in Appendix 1. The results of this evaluation are presented in the form of isotherms in Figures 8-15. The position of the wall and the temperatures at the wall in Figures 8-15 are approximations due to three factors. First, the test cylinder diameter varied slightly along its length. Second, the rubber gaskets were not exactly round and perfect alignment with the cylinder ends was unobtainable due to the simple mounting technique employed. Third, and most important of all is the fact that there is an image duplication of the test section common to all differential interferometers which results in two images of the test cylinder separated by the small beam separation distance ΔX. Through each point in the test section there passes an ordinary and an extraordinary ray. Since each of these rays is diffracted at the last Wollaston Prism, two images appear. These three factors combine to make the location of the wall and the position of the deflected fringes at the wall at best an approximation.

Due to the position of the horizontal fringes no data are available close to either the top or the bottom of the cylinder; however, dashed lines indicate an expected extension of the data obtained.

From all of the Figures 8-15 it is seen that there exists a region close to the wall approzimating pure conduction. The free convec-

tion phenomenon results from a temperature gradient established along the vertical centerline where the colder (denser) region exists at the bottom of the cylinder and the hotter (less dense) region exists at the top of the cylinder.

After approximately thirty minutes the temperature of the water-filled cavity had everywhere asympotically reached that of the wall.

The isotherms for each time were evaluated to obtain the transient bulk temperatures shown in Figure 16. The bulk temperature was defined as the mean temperature obtained from the isotherms by a simple area weighted average of all the isotherms at a given time. The dashed line indicates the expected results in the region between time zero and ninety seconds. The data in this region showed considerable scatter and were therefore discarded.

To obtain a measure of the accuracy of the data an error analysis was performed and is given in Appendix 3. An error in the temperature at a point of $\pm$ 19.0 per cent is directly attributed to differential interferometry as used in this research. An error in the temperature at a point of $\pm$ 7.0 per cent is attributed to the temperature measuring system. The combined error in the temperature at a point is the sum of the above two errors or $\pm$ 26.0 per cent.

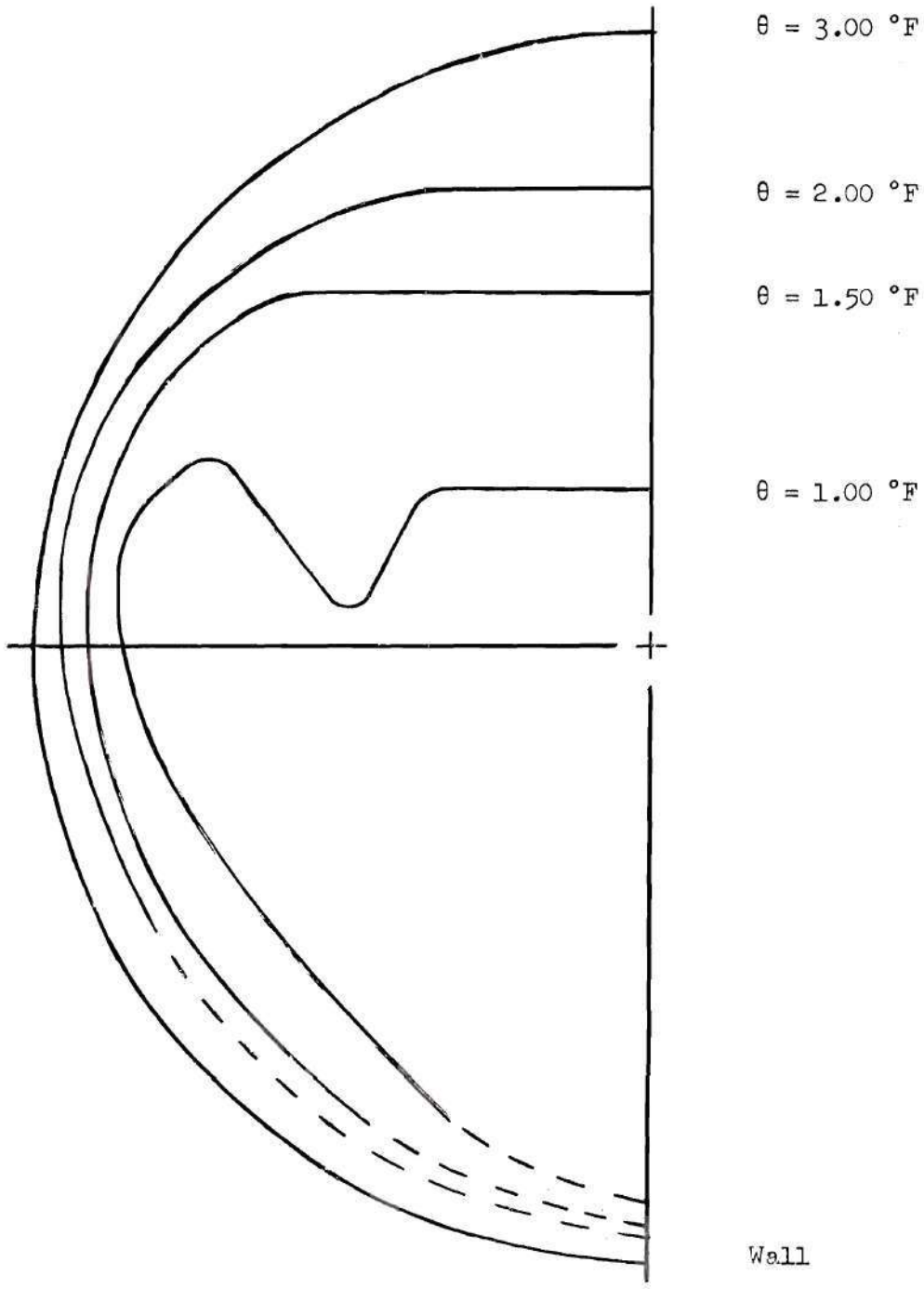

Figure 8. Isotherms — τ = 90 sec.

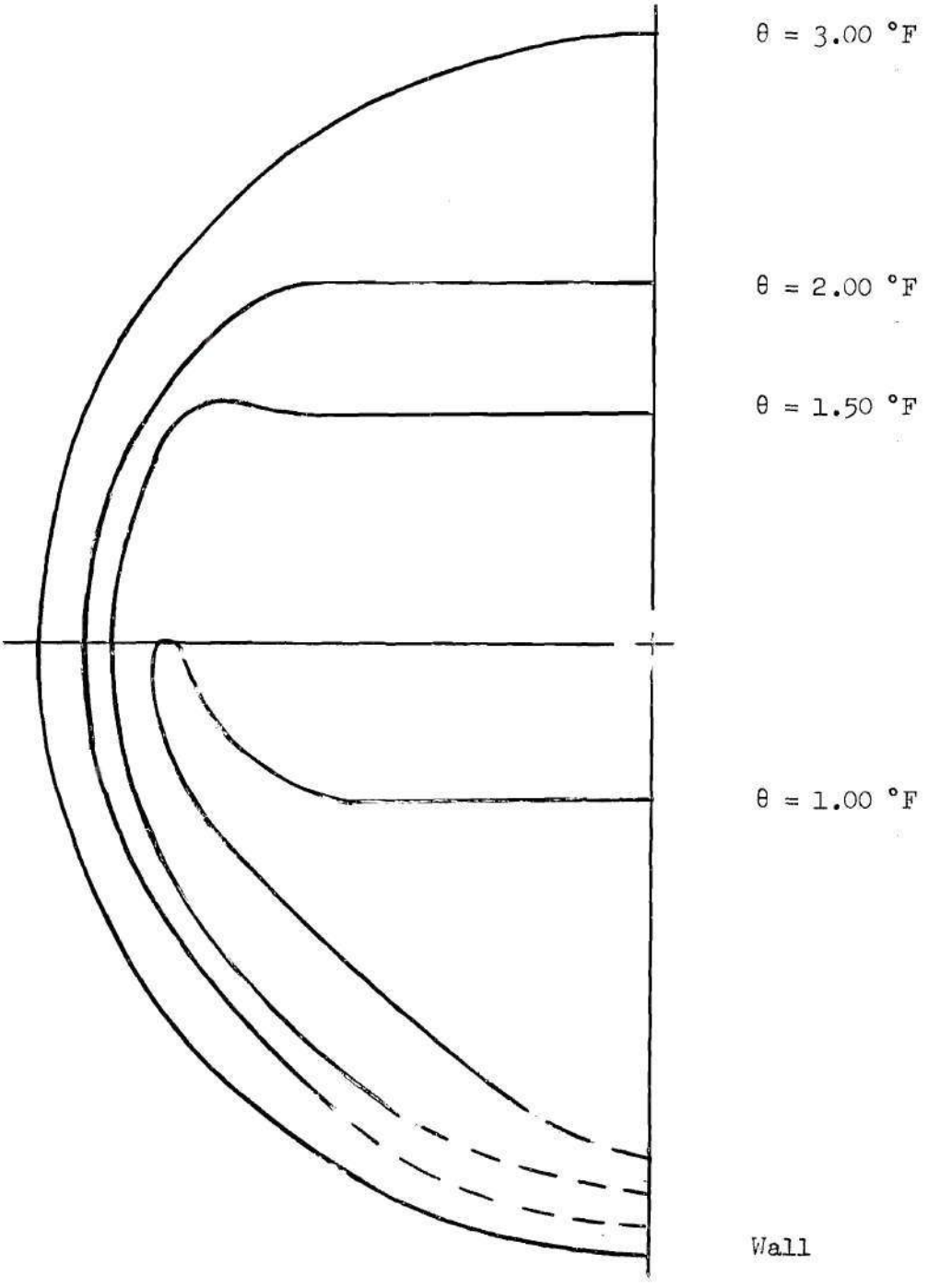

Figure 9. Isotherms — τ = 120 sec.

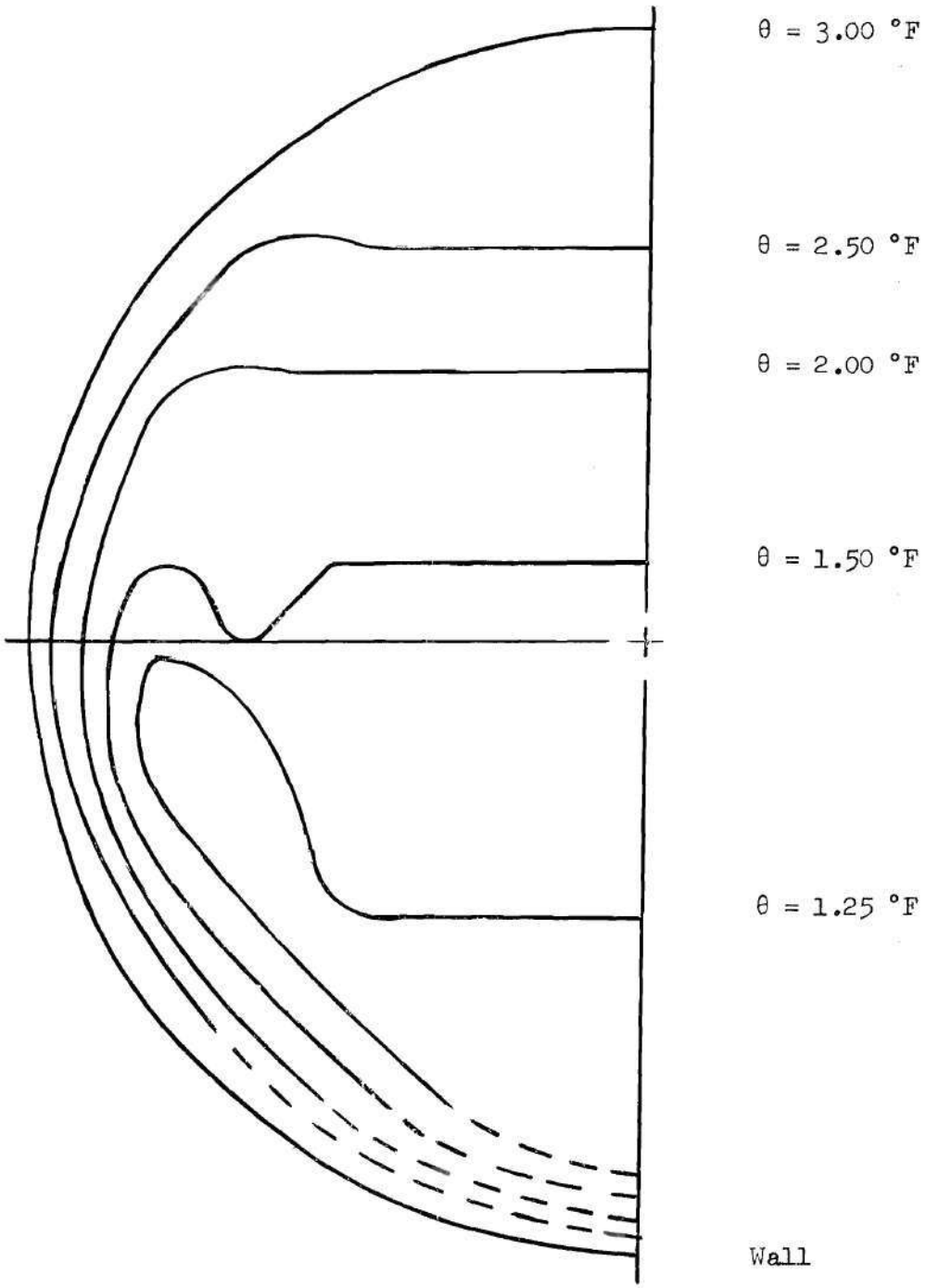

Figure 10. Isotherms – τ = 180 sec.

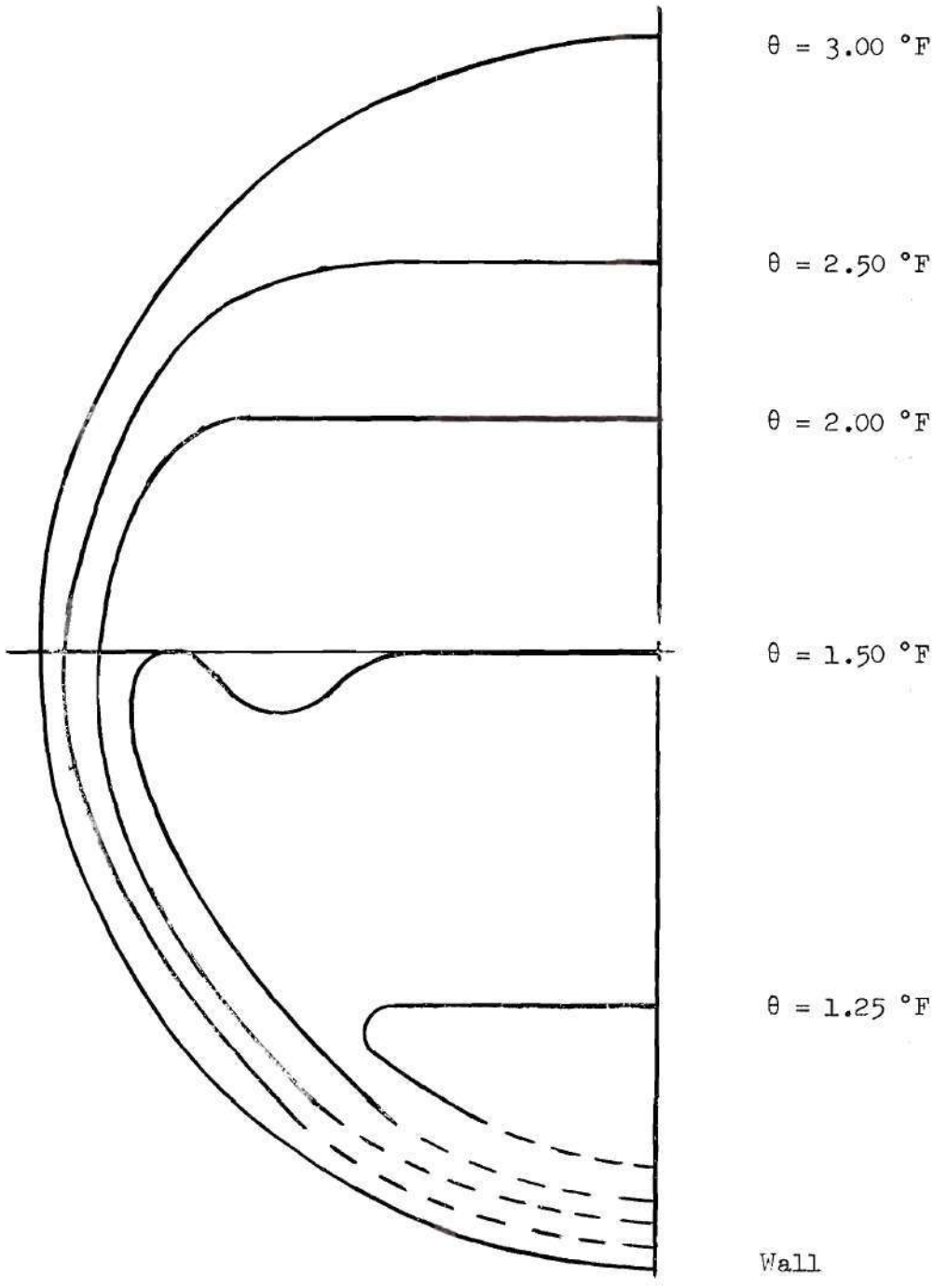

Figure 11. Isotherms – τ = 240 sec.

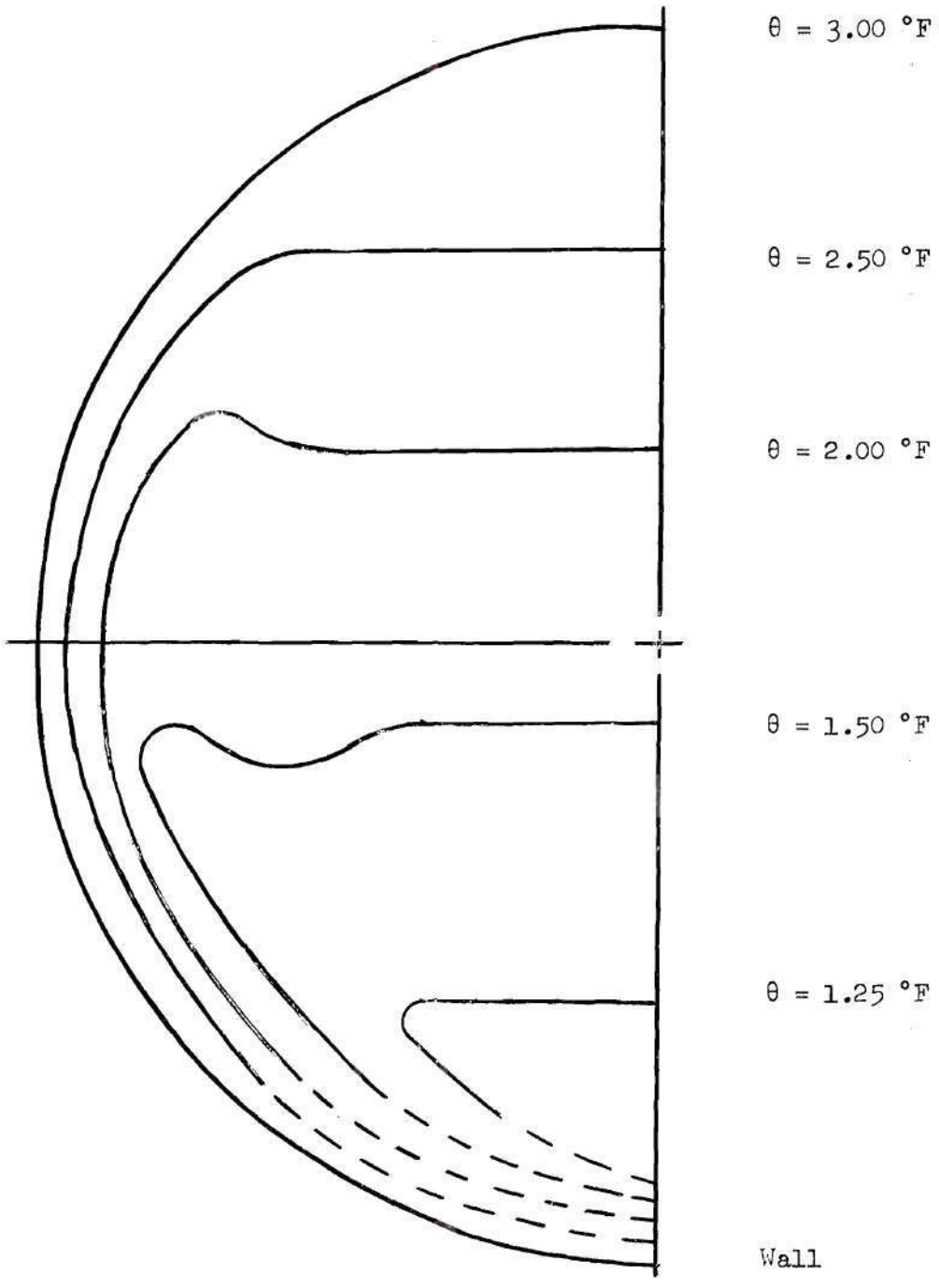

Figure 12. Isotherms — τ = 300 sec.

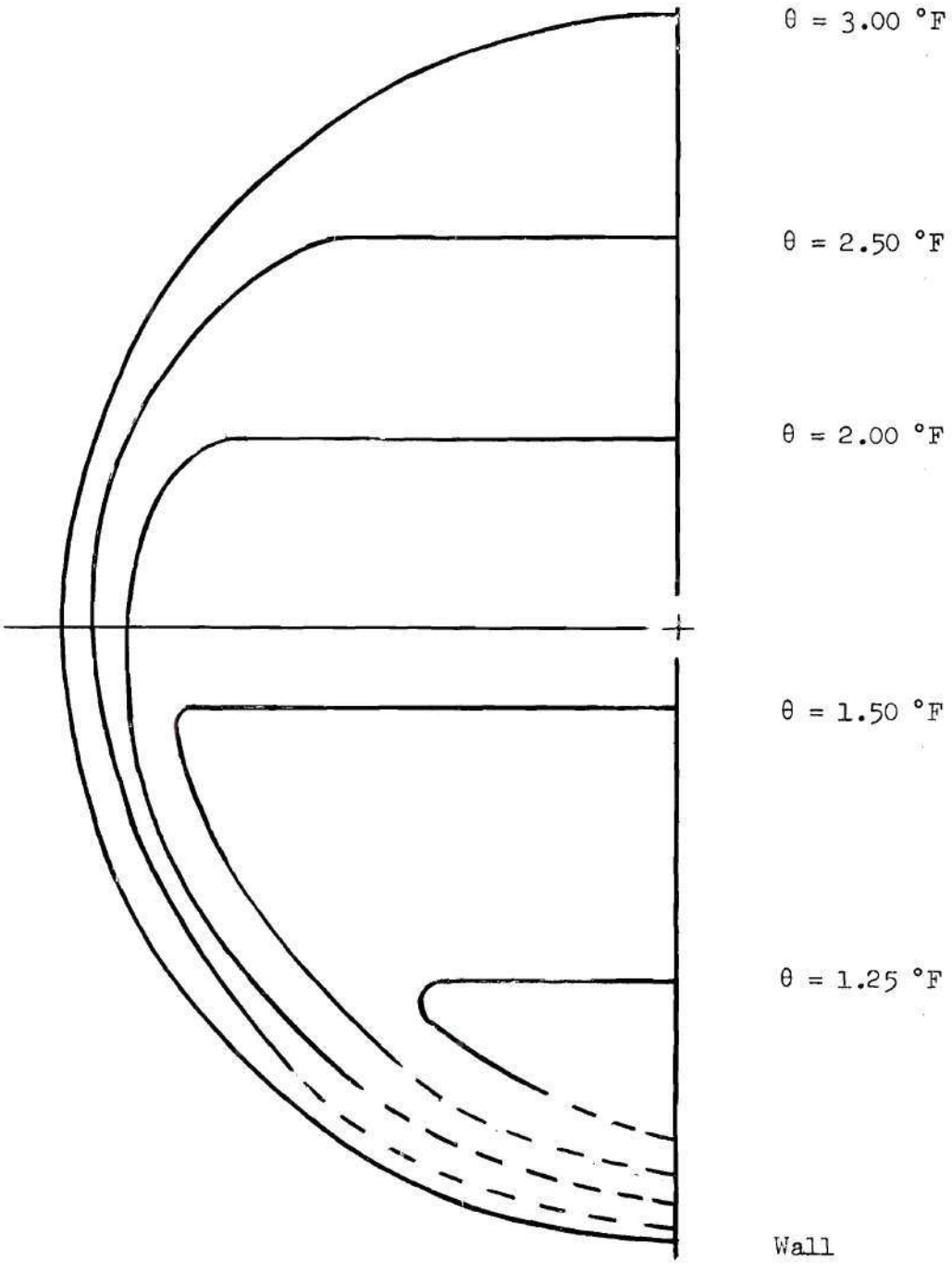

Figure 13. Isotherms — τ = 360 sec.

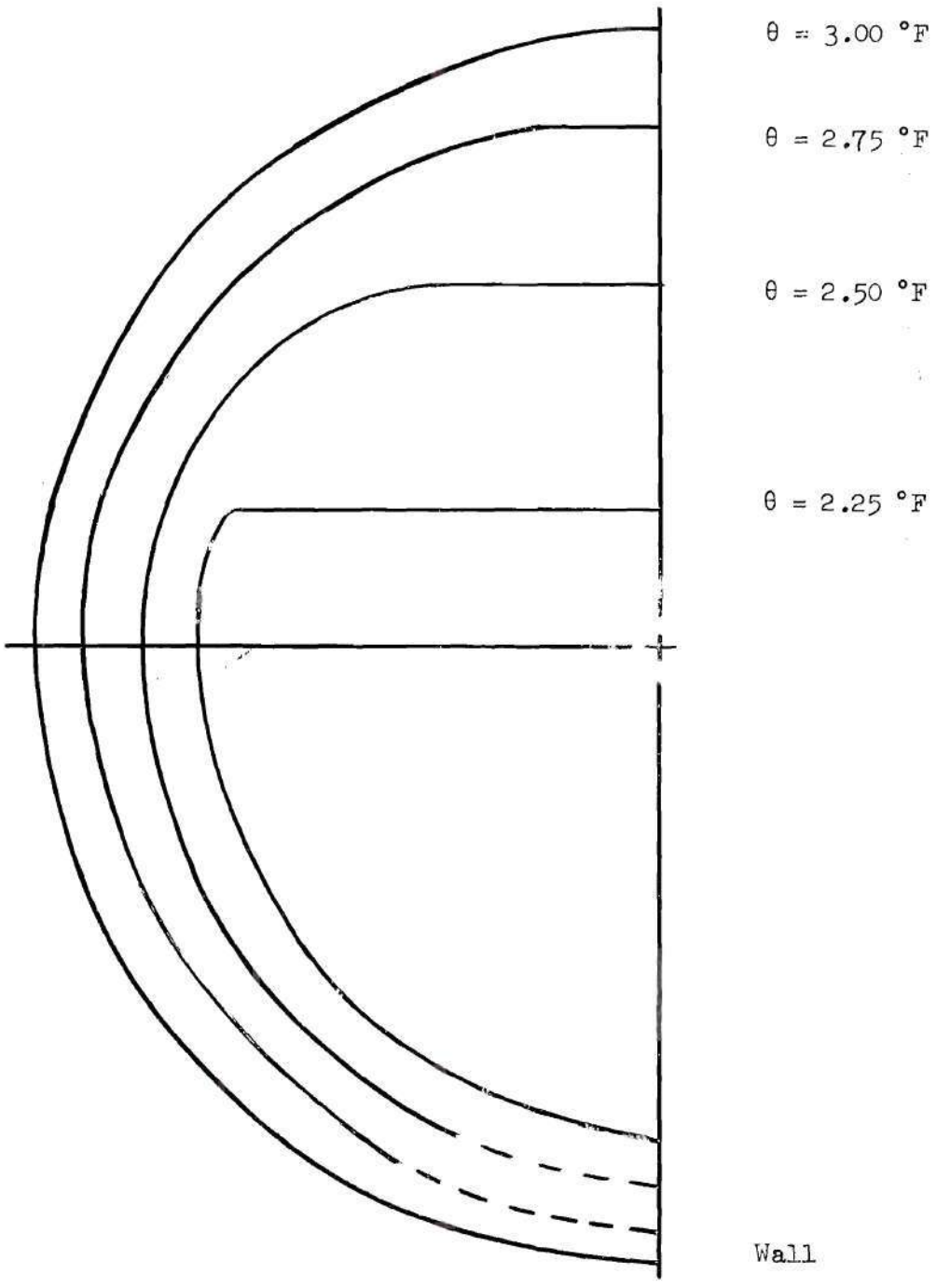

Figure 14. Isotherms – τ = 720 sec.

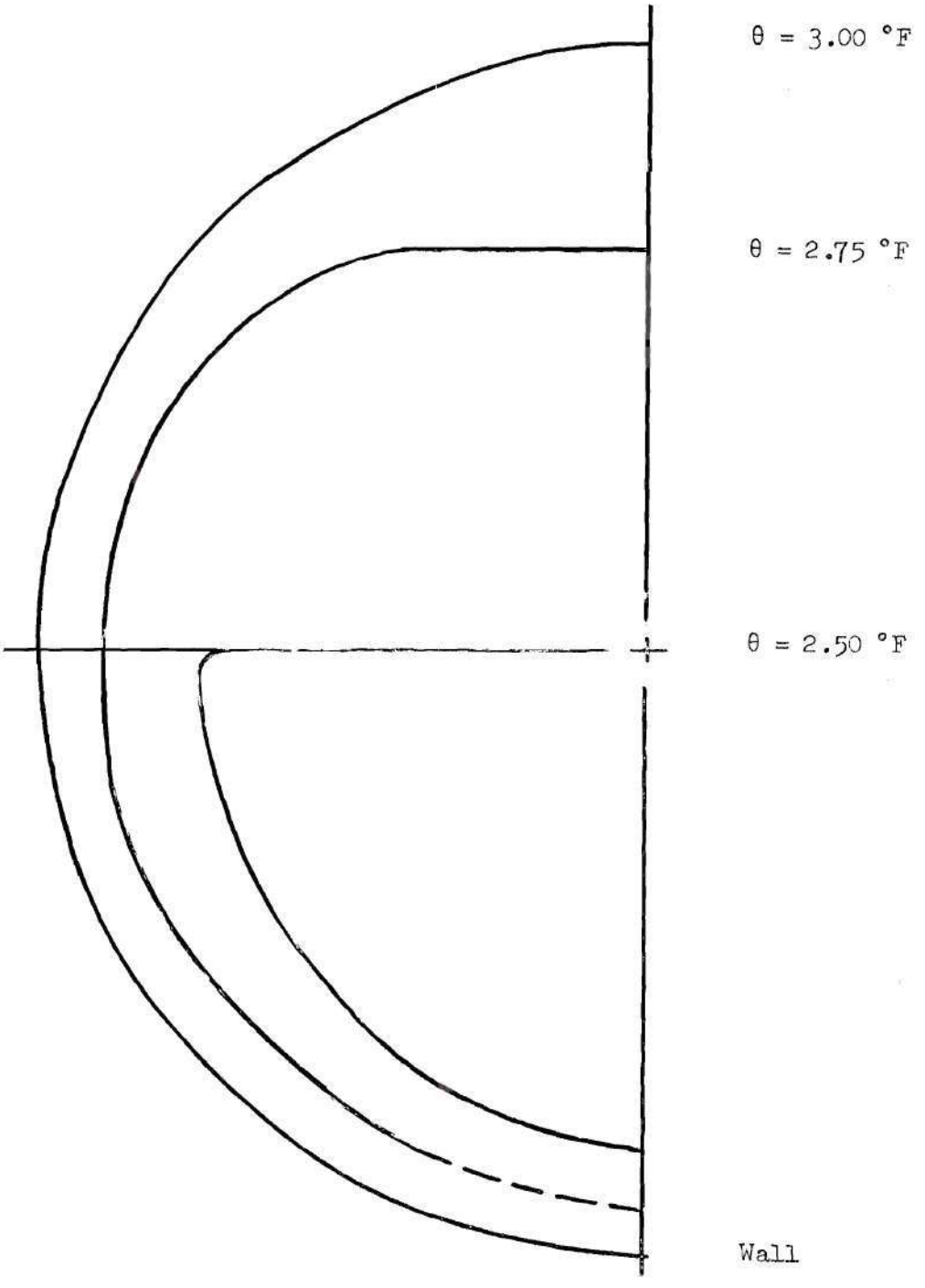

Figure 15. Isotherms – τ = 1200 sec.

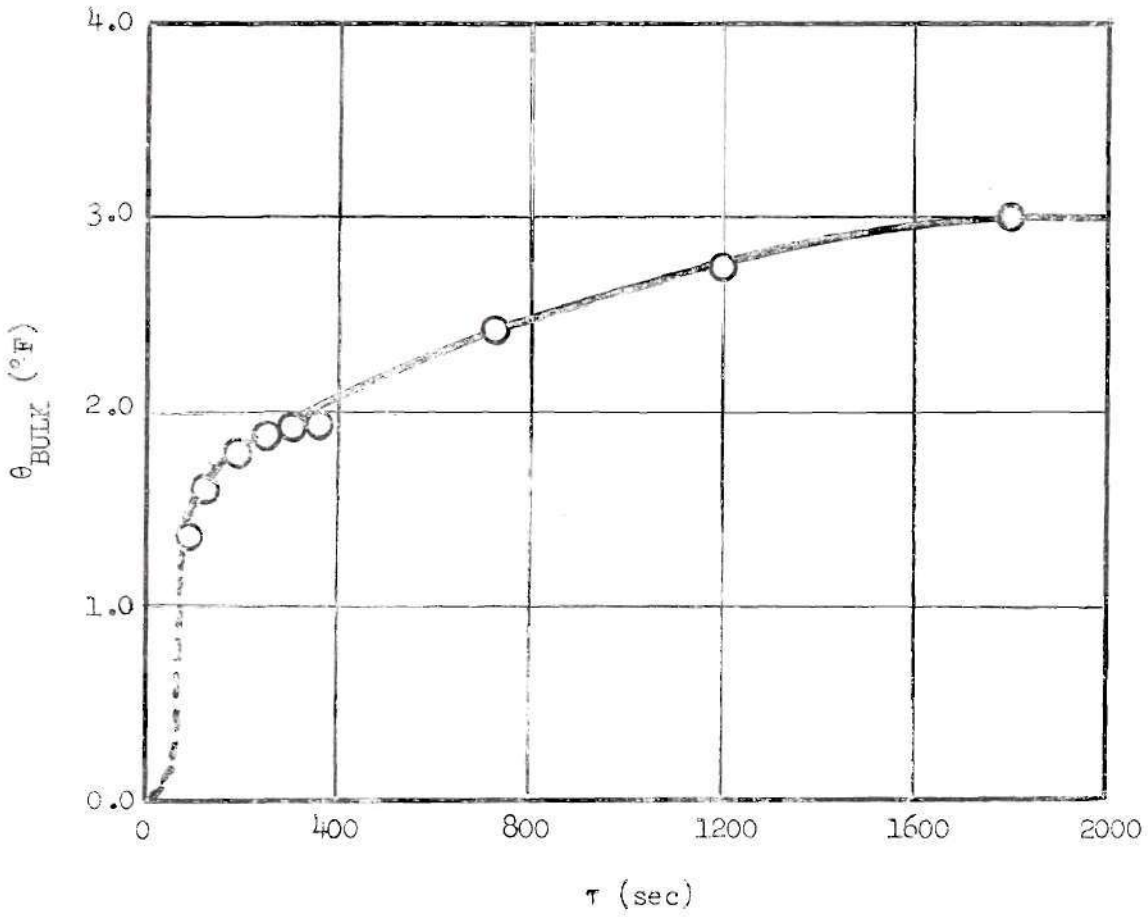

Figure 16. Transient Bulk Temperature

CHAPTER VI

CONCLUSIONS

The results of this research indicate that the differential interferometer can be successfully applied to problems characterized by confining solid boundaries with the possible exception of the region immediately adjacent to the solid boundary.

The new technique for evaluation of the interferograms inside curved, confining, solid boundaries which was derived in this research proved to be valid.

The heat transfer phenomenon exhibited by the horizontal, water-filled cylinder heated at a constant wall temperature different from that of the initial uniform water temperature is characterized by a region close to the wall where the heat transfer process is essentially pure conduction.

The transient phenomenon approaches the state where all the water has reached the temperature of the wall and free convection cases. The free convection ends asymptotically after approximately thirty minutes.

APPENDIX I

REDUCTION OF INTERFEROGRAMS

The first step in the reduction of an interferogram for a time τ was to project the appropriate 35 mm slides (vertical and horizontal interferograms) onto 14 in. x 17 in. pieces of paper and trace the deflected fringe patterns. These tracings became the enlarged interferograms which were reduced in accordance with Equation (12).

All tests were run with the orange filter, λ = 5820 A, prism setting number one, ΔX = 0.001048 ft., and a test cylinder length (ℓ) of 0.979 ft. Evaluation of Equation (12) proceded with the measuring of D on each interferogram and the determining of MF from Equation (7) using the inside diameter of the test cylinder as a known dimension. The vertical interferograms had a D of 0.0756 ft. and a MF of 4.52. The horizontal interferograms had a D of 0.732 ft. and a MF of 4.38. Inserting these constants in Equation (12) yielded

$$n(x)_{VERT.} = 0.0000381 \int_{REF}^{x} y(x)\, dx \qquad (15)$$

for the vertical interferograms, and

$$n(x)_{HORIZ.} = 0.0000405 \int_{REF}^{x} y(x)\, dx \qquad (16)$$

for the horizontal interferograms with the integral being in square inches in both cases.

Both the vertical and horizontal interferograms began ($\tau = 0$) with a $T_{H_2O\text{-}INITIAL}$ of 77°F (25°C). From Table 1 with a λ = 5820 A and a T of 25°C

$$\frac{\Delta n}{\Delta T} = - 0.0001051 \qquad (17)$$

with ΔT in °C. Substitution of Equation (17) into Equations (15) and (16) yields

$$T(x)_{VERT.} = 0.652 \int_{REF}^{x} y(x)\, dx \qquad (18)$$

and

$$T(x)_{HORIZ.} = 0.693 \int_{REF}^{x} y(x)\, dx \qquad (19)$$

with T in °F and the integral in square inches.

The position of the undeflected fringes in both cases was determined by the known shape and constant location of the $T_{H_2O\text{-CENTER}}$ thermocouple. The interferogram for a time τ_1 was positioned on the reference interferogram for time $\tau = 0$ so that the thermocouple shapes matched.

The central fringe of the vertical interferogram for a time τ_1 was evaluated first using the previously determined $T_{H_2O\text{-CENTER}}$ vs. τ, Figure 17, values at the reference boundary (thermocouple tip). This central vertical fringe then formed the reference boundaries for the horizontal fringes at τ_1 which were evaluated next.

Figure 18 is a typical vertical interferogram. The integral in Equation (18) was performed for each τ in twelve increments by a planimeter. Vertical interferograms were evaluated for each photograph listed in Table 4. Results of a typical vertical interferogram evaluation are presented in Figure 19. From these evaluations plots of transient temperatures were derived for each undeflected horizontal fringe position shown in Figure 19, thus serving as reference boundaries in the evaluation of Equation (19) for the horizontal interferograms. A typical transient temperature plot for an undeflected horizontal fringe position is shown in Figure 20.

Figure 21 is a typical horizontal interferogram. The integral in Equation (19) was performed at a given τ for each horizontal fringe in 24 increments by a planimeter. Horizontal interferograms were evaluated at times of 90, 120, 180, 240, 300, 360, 720, and 1200 sec.

For the complete calculations made in reducing the interferograms, contact

Dr. W. O. Carlson
Mechanical Engineering Department
Georgia Institute of Technology
Atlanta, Georgia 30332

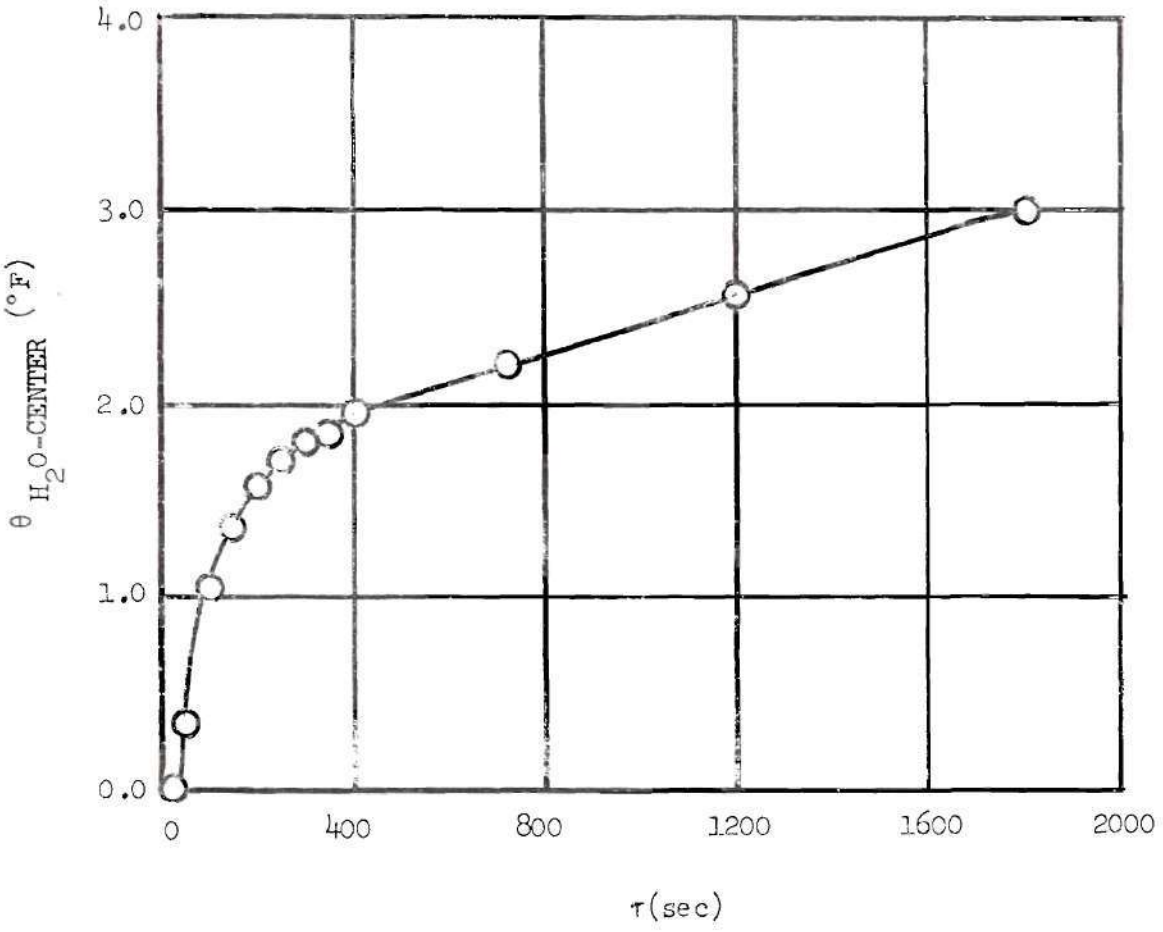

Figure 17. Transient Center Temperature

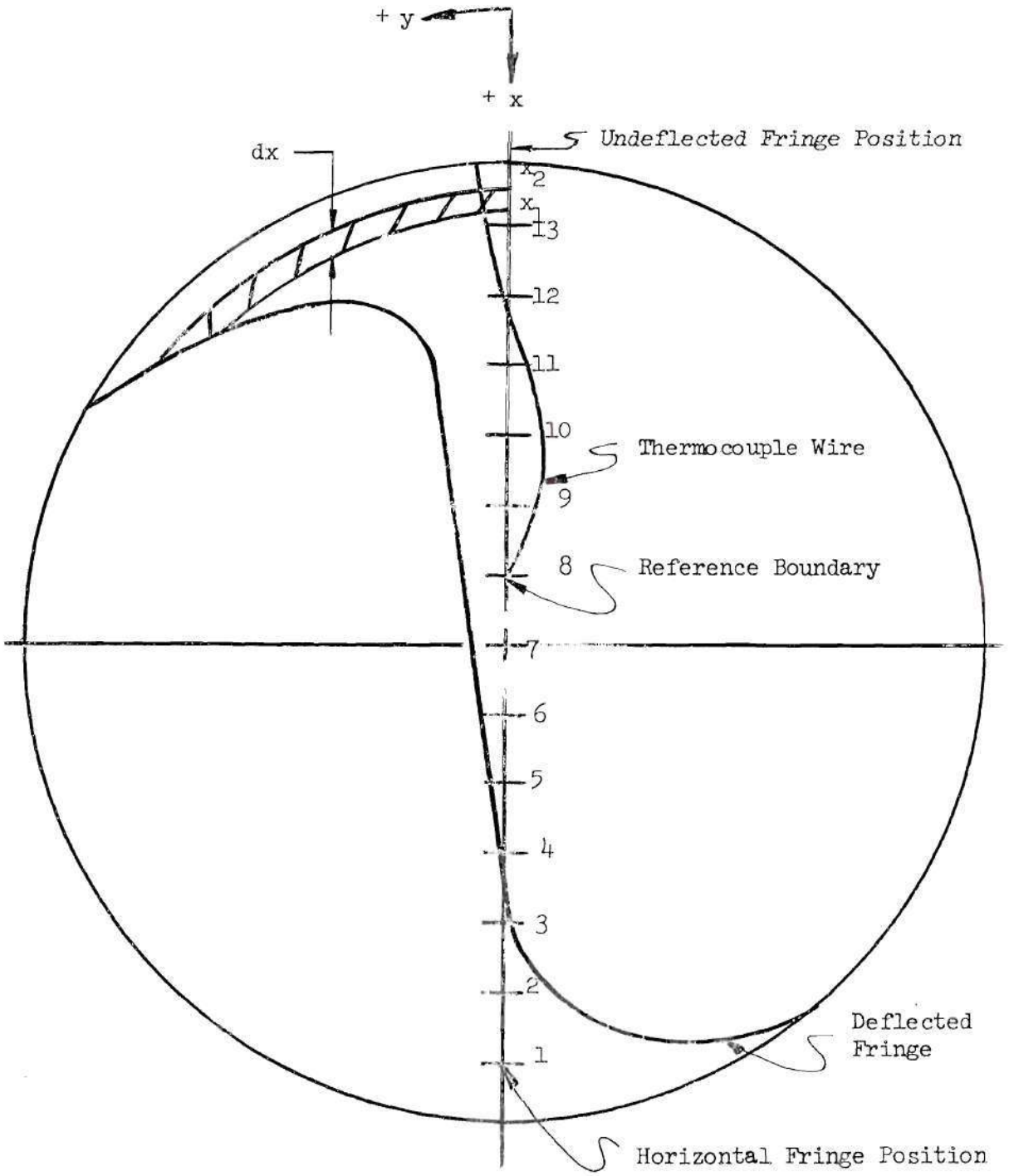

Figure 18. Typical Vertical (90°) Interferogram

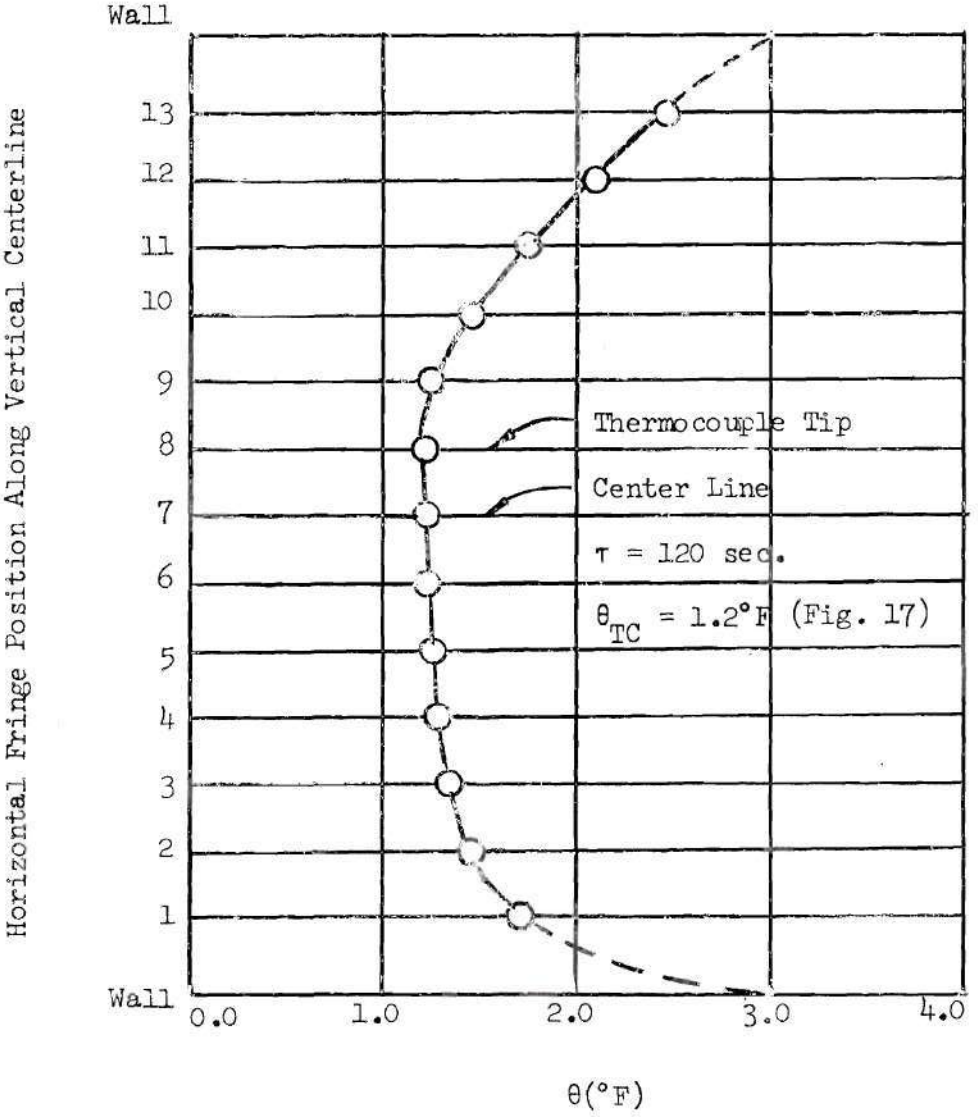

Figure 19. Typical Vertical Interferogram Evaluation Results

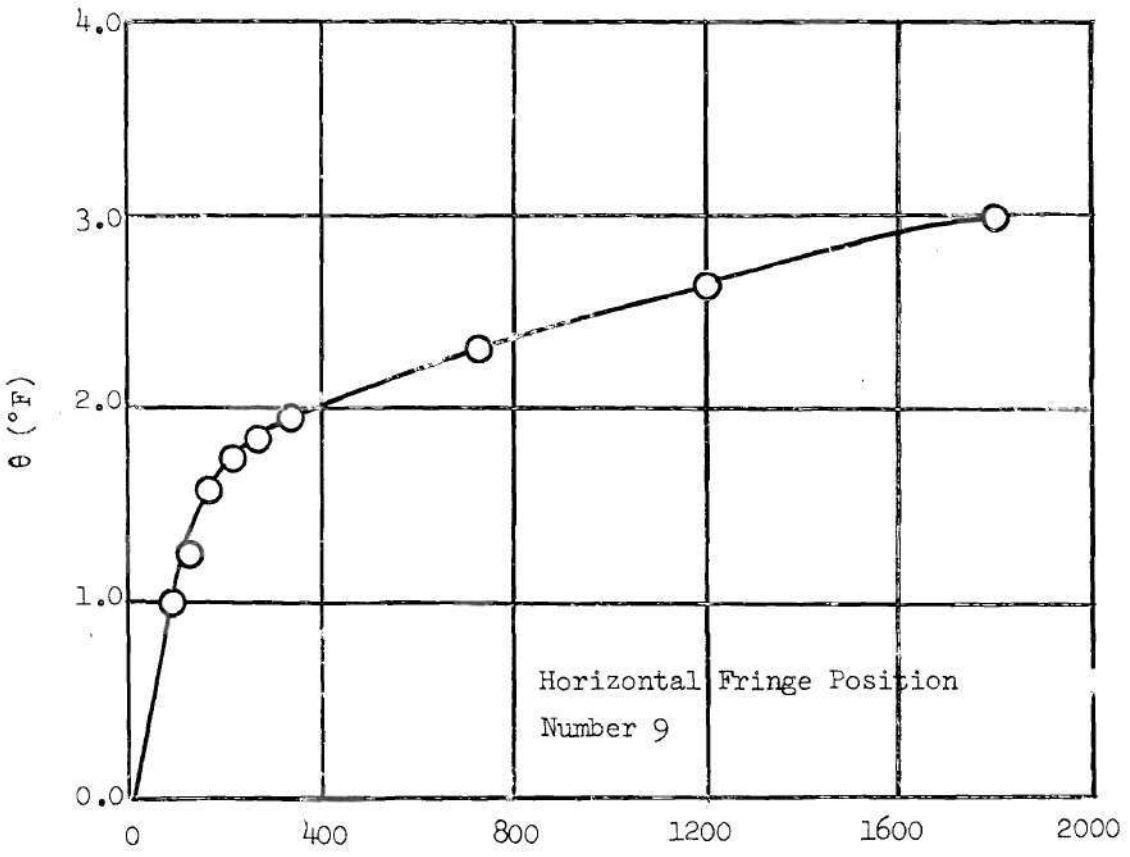

Figure 20. Typical Transient Temperatures at A Horizontal Fringe Position

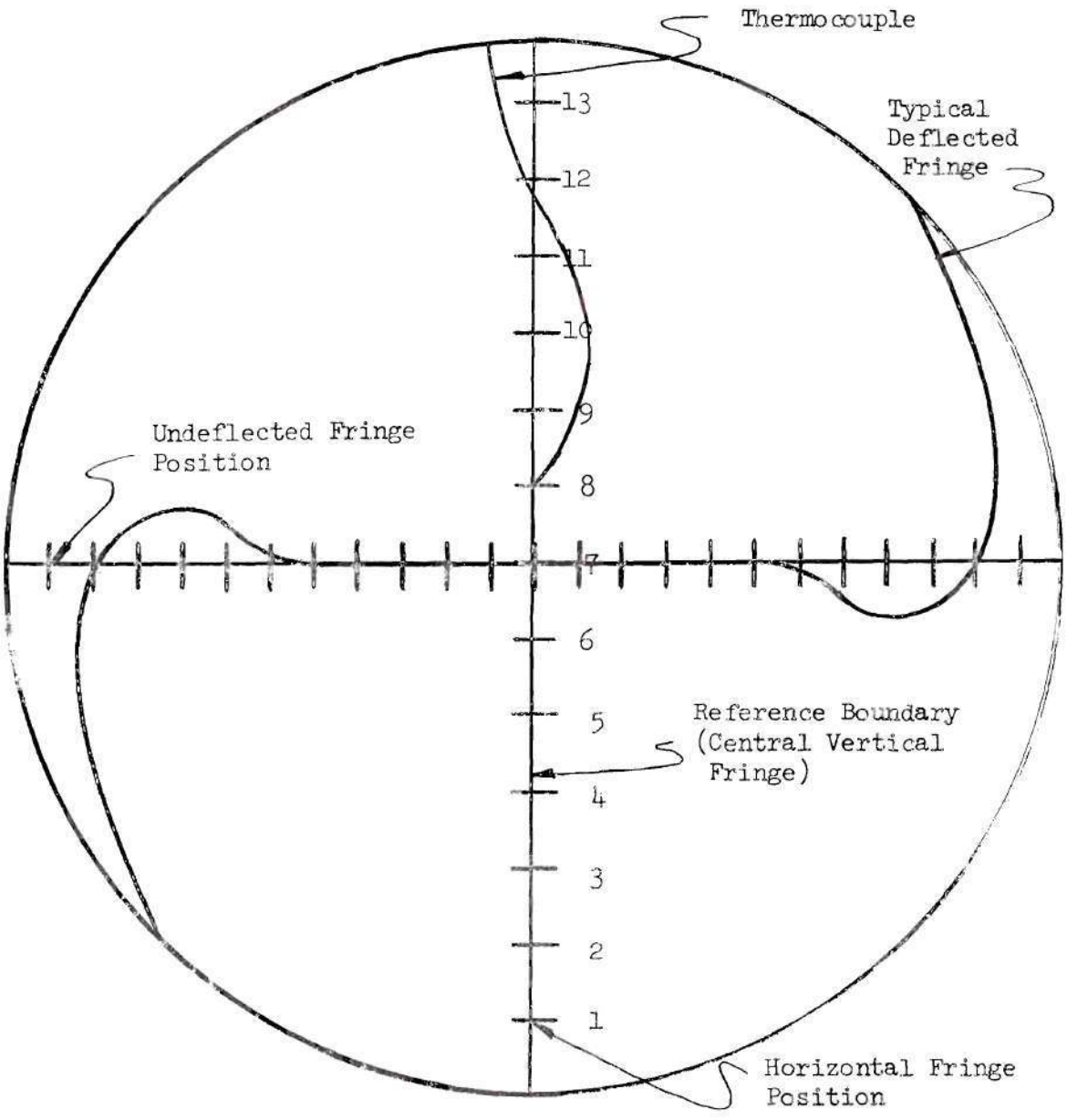

Figure 21. Typical Horizontal (0°) Interferogram

APPENDIX 2

CALIBRATION OF THERMOCOUPLES

The two thermocouples, cylinder wall and center, were calibrated by means of a constant temperature bath and a previously calibrated copper-constantan thermocouple. Each thermocouple was immersed in the bath with the calibrated thermocouple and readings were taken at 74.4°F and 73.0°F.

Both thermocouples exhibited a constant error in the range tested and a constant correction factor was applied to each thermocouple. These correction factors are as follows:

Table 5. Calibration of Thernocouples

Thermocouple	°F
Wall	+ .3
Center	+ .2

APPENDIX 3

ERROR ANALYSIS

An understanding of the errors present in this investigation must be realized before the accuracy of the results can be accepted. The sources of these errors were the standards used for calibration, the reading of the potentiometer, the recording, tracing, and reading of the interferograms, and the constants of the differential interferometer.

The thermocouples were calibrated in a constant temperature bath using a thermocouple which had previously been calibrated using thermometers calibrated by the National Bureau of Standards to $\pm$ 0.18°F. Assuming that the calibration of the reference thermocouple was as accurate as that of the National Bureau of Standards an error of $\pm$ 0.18°F of $\pm$ 6.0 per center of the temperature difference between the wall and the cylinder center, θ_w = 3.0°F, was assumed. An error in reading the potentiometer was assumed with an estimated deviation of $\pm$ 0.0025 mv. or $\pm$ 1.0 per cent.

The photographic system induced at $\pm$ 4.0 per cent reduction in diameter along the vertical centerline of the cylinder. Tracing and reading of the interferograms were assumed accurate to 1/8 in. on a 12 in. enlargement of the interferogram for an accuracy of $\pm$ 1.0 per cent. With the $\pm$ 4.0 per cent reduction in diameter along the vertical center line and the $\pm$ 1.0 per cent error tracing and reading the interferograms, D, MF, and y(x) in Equation (12) are accurate to $\pm$ 5.0 per cent.

The instrument constants in Equation (12) and λ and ΔX. λ according to Table 2 is accurate to $\pm$ 75 Å or $\pm$ 1.3 per cent for the orange filter. ΔX was assumed accurate to $\pm$ 0.5 per cent as was ℓ, the test cylinder length.

For the worst case conditions, Equation (12) predicts a $\pm$ 19.0 per center variation in temperature.

This differential interferometry error of $\pm$ 19.0 per cent when combined with the $\pm$ 7.0 per cent error induced by the temperature measuring system produces an overall error in the measurement of the temperature, θ, at a point of $\pm$ 26.0 per cent.

BIBLIOGRAPHY

1. Renet, C., "Strioscopic Quantitive En Soufflerie," O.N.E.R.A. Note Technique No. 23 (1954).

2. Philbert, M., "Emploi De La Strioscopie Interferentielle En Aerodynamique," La Recherche Aeronautique, vol. 65, p. 19, (1958).

3. Waterhouse, J. F., Wilby, P. Spencer, H. B. and Morton, D., "Application of the Schlieren - Interferometer to the Study of Flow About a 2-Dimensional Wedge at Supersonic Speeds," unpublished theses, College of Aeronautics, Cranfield, England, July, 1959, July, 1960.

4. Waterhouse, J. F. and Spencer, H. B., "The Application of the Schlieren-Interferometer to the Study of Supersonic Flow Around Unyawed Axi-Symmetric Bodies," Royal Aeronautical Society, vol. 65, p. 691 (1961).

5. Chevalerias, R., Latron, Y., and Veret, C., "Methods of Interferometry Applied to the Visualization of Flow in Wind Tunnels," Journal of the Optical Society of America, vol. 47, No. 8, p. 703 (1957).

6. Gontier, G., "Contribution A L'Etude De L'Interferometer Differential A Biprisme De Wollaston," Publications Scientifiques Et Techniques Du Ministere De L'Air, No. 338 (1957).

7. Solignac, J. L., "Examples D'Application Des Methodes De Mesures Optiques A Des Recherches Fondamentales F'Aerodynamique," Organisation Du Traite De Consultatif Pour La Recherche Les Realsations Aeronautiques, Rapport 398.

8. Oertel, H., "Differentialinterferenzaufnahmen Kurzzeitiger Hyperschallstromunger," Kino-Technik, No. 2, p. 29 (1962).

9. Smeets, G., "Differential Interferometer for Observing and Measuring Boundary Layers," Note Technique-Technische Mitteilung, September 2, 1964.

10. Kramer, C. and Naumann, A., "Die Differentialinterferometric als Mesverfahren der Gasdynanischen Forschung," Transactions of the Rhein-Westphallian Technical Univ. in Aachen, vol. 18 (1965).

11. Mordchelles-Regnier, G., and Kaplan, C., "Visualization of Natural Convection on a Plane Wall and in a Vertical Gap by Differential Interferometry. Transitional and Turbulent Regimes," Proceedings of the Heat Transfer and Fluid Mechanics Institute, Stanford University Press, p. 94 (1963).

12. Lamb, J. D. and Schreiber, P. W., "The Application of a Differential Interferometer to an Axially Symmetric Arc Headed Plasma," Aerospace Research Laboratories, No. ARL 66-0222, November, 1966.

13. Hellums, J. D. and Churchill, S. W., "Transient and Steady State, Free and Natural Convection, Numerical Solutions," American Institute of Chemical Engineering Journal, vol. 8, No. 5, p. 692 (1962).

14. Martini, W. R., and Churchill, S. W., "Natural Convection Inside a Horizontal Cylinder," A.I.Ch.E. Journal, vol. 6, No. 2, p. 251 (1960).

15. Wilkie, D., and Fisher, S.A., "Measurement of Temperature by Mach-Zehnder Interferometry," Proceedings of the Institute of Mechanical Engineers, vol. 178, pt. 1, no. 17, p. 461.

16. Weinberg, F. J., Optics of Flames, p. 23, Washington, Butterworths, 1963.

17. Dorsey, N. E., Properties of Ordinary Water-Substance, p. 281 New York, Rheinhold Publishing Corp., 1940.

18. Halliday, D. and Resnick, R., Physics for Students of Science and Engineering, New York, Wiley and Sons, Inc., 1962.

19. Schrader. W., "Differential Interferometer," Feinmechanik und Optik, Wenden bie Braunschweig, West Germany.